University of Alberta
Printing Department

THE UNIVERSITY OF ALBERTA

"A THEORETICAL AND EXPERIMENTAL INVESTIGATION OF THE KNOOP HARDNESS"

by

WAYNE E. NYSETVOLD, B.Sc. (Alberta)

A THESIS

SUBMITTED TO THE FACULTY OF GRADUATE STUDIES

IN PARTIAL FULFILMENT OF THE REQUIREMENTS

FOR THE DEGREE OF MASTER OF SCIENCE

DEPARTMENT OF MECHANICAL ENGINEERING

EDMONTON, ALBERTA

APRIL, 1964

ABSTRACT

The purpose of this thesis is to investigate the application of plane strain plasticity theory to the analysis of the Knoop hardness test.

The theory presented is compared with experiments performed on superpure aluminum, work hardened 0.06% tellurium lead, annealed 0.06% tellurium lead, and annealed 0.2% carbon mild steel. The maximum Knoop diagonal length produced in the experiments is 1.3600 inches.

It is shown that the theory, developed for a rigid-plastic model, agrees closely with experimental results obtained from one of the metals studied. This metal, work hardened 0.06% tellurium lead, has a stress-strain curve approximating that of a rigid-plastic non-hardening solid.

In determining the stress-strain curves for the metals studied, the Taylor method and Ford's modification of the Cook and Larke method are compared and recommendations are made.

ACKNOWLEDGEMENTS

The author wishes to extend his appreciation to Dr. J. B. Haddow for his supervision and guidance of this thesis.

Additional thanks are extended to the Department of Mechanical Engineering for making his graduate studies possible.

He expresses thanks to H. Golls for his helpfulness in preparing the test apparatus and specimens.

He would also like to thank his wife, Ione, for her consideration and encouragement.

Thanks is expressed to the Aluminum Company of Canada for supplying the aluminum used in the experimental work.

TABLE OF CONTENTS

LIST OF TABLES

LIST OF FIGURES

FIGURE PAGE

CHAPTER 1

HARDNESS TESTING

Hardness is an elusive quantity[1,2] that in general implies a resistance to penetration. This suggests, for example, that steel is harder than rubber. Hardness may also be thought of as a measure of the resistance to permanent deformation, and in this suggests that rubber is harder than steel. This latter concept indicates that for some materials, elastic properties play a very large part in the determination of hardness. Since the elastic strains in metals are usually small compared with the plastic strains when a metal is penetrated by an indenter, (in order to assess its hardness) the hardness properties of a metal are largely determined by the plastic characteristics of that metal.

Hardness may be measured in three ways: by scratching, by indentation, and by dynamic methods. In dynamic hardness testing, the elastic properties of a metal may be as important as the plastic properties.

1.1 SCRATCH HARDNESS

Mineralogists first developed this method based on the

ability of one solid to scratch the other. Mohs (1822) gave it a qualitative basis by selecting ten minerals to be used as standards of hardness. This scale, based on talc with a scratch hardness of one to diamond with a scratch hardness of 10, is useful when a wide range of materials is considered but the harder metals fall between 4 and 8, so the divisions are not suited to them. Another disadvantage of this method of determining the hardness of a material is that the values obtained may depend on the orientation of the scratching edge.

1.2 DYNAMIC HARDNESS

A dynamic hardness value is obtained by a measurement of the energy lost by an object of specified geometry, when it impinges with a given velocity on the material. In the Shore Rebound Scleroscope (Shore 1918) the hardness is measured in terms of the rebound of the indenter. This method has the advantage that the hardness of large machine parts may be measured without moving them.

1.3 STATIC INDENTATION HARDNESS

Static indentation measurements of hardness are the most widely used and accepted today. The methods all involve the formation by a static load of a permanent deformation (indentation) in the surface of a material. The hardness is a

function of the load applied, and the geometry of the indentation and or the indenter.

A short discussion of some of the common methods of indentation hardness testing is now given.

1.3.1 BRINELL HARDNESS

In the Brinell hardness test, (Brinell 1900) a hard spherical indenter is pressed by a fixed normal load into the specimen. The hardness number is expressed as the ratio of the load to the curved area of the indentation. This method of hardness measurement has an obvious disadvantage in that geometric similarity is not preserved as the load is increased. Thus, the B.H.N. is dependent on load and indenter size.

Meyer showed that for a given ball used in the Brinell test, and using different loads on a given specimen,

$$L = ad^n$$

where L is the load, d is the diameter of the impression, and a and n are constants for a given material. Meyer demonstrated that the exponent n was related to the work hardening capacity of the metal. For materials in the annealed condition, n is between 2.5 and 3.0 but in the fully work hardened state, n approaches 2.

In 1908, Meyer suggested taking the ratio of the applied load to the projected area of the impression as a hardness measurement (now called the Meyer hardness). This concept does not change the indenter characteristics; therefore it is subject to the disadvantages of the Brinell test. In addition it is

difficult to measure the chordal diameter of the impression because of the phenomena of "piling up" and "sinking in" illustrated in Figure 1.

(a) (b)

FIGURE 1: (a) Piling up: observed with highly work hardened materials. (b) Sinking in: observed with annealed materials.

1.3.2 ROCKWELL HARDNESS

This test uses either a steel ball one sixteenth inch in diameter loaded with 100 kg (scale B) or a diamond cone loaded with 150 kg and having a 120 degree included angle (scale C). The depth of indentation is registered as a Rockwell number. The Rockwell test is particularly useful for rapid routine measurements on finished products.

1.3.3 VICKERS HARDNESS

In the Vickers test, a square based pyramid with included angles of 136 degrees is loaded normal to the test specimen. A microscope measuring device is used to measure the diagonals, and the Vickers hardness is determined by dividing the load by the contact area of the impression.

In this test, the condition of continuing geometric similarity is satisfied. However, the diagonals must be measured after the indenter is withdrawn so some elastic recovery is inevitable, here as well as in the other tests mentioned. The Brinell and Vickers hardness are approximately equal up to values of 300 kg/mm^2 but the Brinell number is not reliable above 600.

1.3.4 KNOOP HARDNESS

In the development of indentation methods, many shapes of indenters have been investigated, but only the ones such as the ball, cone and square based pyramid forms, which yield symmetric indentations have received general acceptance. These shapes have the inherent strength necessary to withstand the loads required to give an indentation of accurately measureable size, but are of little value in the testing of brittle materials such as glass, the investigation of surface characteristics, or the measurement of hardness of metal films.

In 1939, Knoop, Peters, and Emerson[3] published results obtained with a variety of elongated pyramidal shaped indenting tools, and attributed mid-nineteeth century use of the regular pyramid with diamond shaped (rhomb) base to Major W. Wade[4] for testing the hardness of cast iron and to T. J. Rodman[5] for use of the test in measuring the pressure of a gas in the bore of a gun.

Wade and Rodman obtained excellent results, but restricted dissemination of their data accounts for the lack

of immediate further development of the elongated pyramidal indenter. Smith and Sandland[6] used the indenting diamond ground to the shape of a square based pyramid.

Knoop[7] suggests, "Results obtained with diamond indenting tools of the elongated pyramidal shape* indicate that this indenter deserves greater recognition in that (1) it makes possible accurate measurements of unrecovered indentations, (2) it extends the application of indentation tests to glass, and other brittle materials as well as to specimens of small size, and (3) it permits a better understanding and possible evaluation of elastic recovery and other physical properties which are involved in indentation measurements".

Using these reasons as a basis, several different geometrical forms of the elongated pyramidal indenter were investigated and it was concluded that the optimum geometry is as illustrated in Figure 2.

This indenter produces an indentation of length, $2\ L_o$, which is about seven times the width, w, and thirty times the depth, C_o.

---

* Hardness Testing Device, - U.S. PATENT NO. 2091995 issued to Frederick Knoop and assigned by him to the U.S. Government.

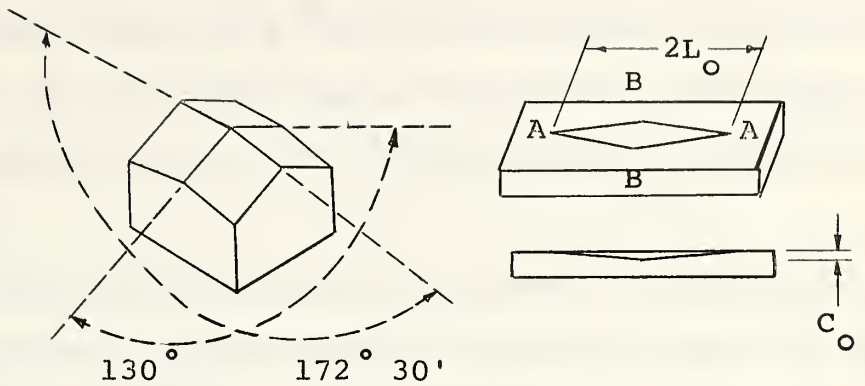

FIGURE 2 THE GEOMETRY OF THE KNOOP INDENTER

By examination of indentations in transparent materials in polarized light, Knoop substantiated his claims that a specimen under load will be greatly strained at BB and relatively unstrained beyond AA. He also states that "the major part of the elastic recovery of an indentation upon removal of the indenter will take place crosswise rather than lengthwise of the indentation".[8] From this statement, it was reasoned that measurement of the long diagonal, and the use of the associated area would give an unrecovered hardness number.

Tate[9] found that the Knoop number as given above, is consistently higher for low loads than for high loads and reasoned that the material at the ends AA of the indentation must have some elastic recovery. The Knoop indentation geometry is independent of the load, so the shortening of the diagonals

due to elastic recovery should be independent of the indenting load also. The amount of recovery, if it were constant for a given material, would be a higher percentage of the diagonal measurements at low loads than at high loads. The higher Knoop numbers observed at low loads could possibly be explained in this manner.

By measuring the elastic recovery of the diagonal in a glass specimen, Tate arrived at a recovery factor of about 5 microns. That is, the length of the indentation decreased by 5 microns when the load was removed. The recovery factor was added to the measured recovered diagonals for all loads and the resulting Knoop numbers were very nearly independent of load.

Tarasov and Thibault[10] generalize on Tates work by showing how "a constant length correction is found by trial and error which, when added to the measured indentation lengths, results in essentially the same hardness number for each of the loads". Their length correction embodied a part to account for elastic recovery, and a part to account for a visibility error dependent on the optical equipment used.

Recent criticism of the idea of a constant recovery factor comes from Mott[11] who says, "....elastic recovery does occur, but their (Tate et al) conclusions that the diagonal contraction is independent of the size of indentation is open to severe criticism". A dimensional analysis of the indentation problem is given by Woodrow[12] and it demonstrates an expected constancy of unrecovered hardness number with load and indentation size. In the analysis, the unrecovered diagonal was used

but this could just as well have been replaced by the length of the diagonal in the recovered indentation. The hardness number based on the recovered diagonal should therefore be independent of the indentation size. This implies that the recovery factor must be proportional to the unrecovered diagonal. A recovery factor or recovery length that is proportional to the indentation size is more probable than one of constant size as it implies zero recovery for zero indentation.

1.4 CONSIDERATIONS FOR THIS THESIS

The ball, cone, and square based pyramidal indenters and their associated indentations cannot at present be analysed by the methods of the theory of plasticity, but the Knoop indentation can be considered, at least to a first approximation, by the theory of plane strain wedge indentation. An examination of this relationship is studied in this thesis.

CHAPTER 2

PLANE STRAIN WEDGE INDENTATION AND ITS APPLICATION TO THE KNOOP TEST

2.1 THE ASSUMPTION OF A RIGID-PLASTIC MATERIAL

The order of magnitude of the elastic parts of the strains in any plastic deformation of a metal, is 10^{-3} and in plane strain wedge indentation, the order of magnitude of the mean plastic strain is 0.3. Consequently, the elastic strains can be neglected and a rigid-plastic material can be assumed.

2.2 PLANE STRAIN EQUATIONS

The conditions for plane strain are:

(1) flow is everywhere parallel to a given plane (say the (x,y) plane) and,

(2) the motion is independent of the third cartesian co-ordinate, z.

Assuming that there is no plastic volume change ($de^p_{ii} = 0$) each distortion in a state of plane strain consists of a pure shear.

The stress σ_z normal to the (x,y) plane is then -p and the other principal stresses are $-p \pm \tau$ where τ is the shear stress giving the radius of the Mohr circle for stresses at a particular point.

$$\sigma_z = \frac{1}{2} (\sigma_x + \sigma_y) \quad \ldots\ldots\ldots\ldots\ldots\ldots (1)$$

If work hardening is absent, and the hydrostatic pressure, p, does not affect the yield point, then $\tau = k$ where k, the yield stress in pure shear, depends on the yield criterion chosen.

If k is given the proper value, the two most widely accepted yield criteria can be represented by the equation:

$$\tau^2 = \frac{1}{4} (\sigma_x - \sigma_y)^2 + (\tau_{xy})^2 = k^2 \quad \ldots\ldots\ldots\ldots (2)$$

For the Tresca criterion, $k = Y/2$, and for the Mises criterion, $k = Y/\sqrt{3}$, where Y is the uniaxial yield stress.

If quasi-static conditions exist, the equations of equilibrium are:

$$\frac{\partial \sigma_x}{\partial x} + \frac{\partial \tau_{yx}}{\partial y} = 0 \text{ , and } \frac{\partial \tau_{yx}}{\partial x} + \frac{\partial \sigma_y}{\partial y} = 0 \quad \ldots\ldots\ldots (3)$$

The continuity equation is:

$$\frac{\partial U_x}{\partial x} + \frac{\partial V_y}{\partial y} = 0 \quad \ldots\ldots\ldots\ldots\ldots\ldots (4)$$

where U_x and V_y are the x and y components of velocity.* For

---

* In ideal plasticity, viscous effects are neglected and provided inertia forces are also neglected, the stresses are independent of the rate of deformation. Velocities and strain rates may be referred to time or to any other monotonically varying parameter.

an isotropic solid, the principal axes of stress and plastic strain rate coincide, that is:

$$\frac{2\tau_{xy}}{\sigma_x - \sigma_y} = \frac{\frac{\partial U_x}{\partial y} + \frac{\partial V_y}{\partial x}}{\frac{\partial U_x}{\partial x} - \frac{\partial V_y}{\partial y}} \qquad \text{.....(5)}$$

There are five unknowns, σ_x, σ_y, τ_{xy}, U_x, and V_y in equations (2), (3), (4), and (5). Saint Venant first derived these in 1870 and they are the basis for the calculation of stress and strain distribution in the plastic zone.

2.3 CURVILINEAR CO-ORDINATES FOR PLANE STRAIN: CHARACTERISTICS AND SLIP LINES

To introduce the concept of characteristics of partial differential equations, introduce the variables p and ϕ such that: (See Figure 3)

$$\begin{aligned} \sigma_x &= -p - k \sin 2\phi \\ \sigma_y &= -p + k \sin 2\phi \qquad \text{.....(6)} \\ \tau_{xy} &= k \cos 2\phi \end{aligned}$$

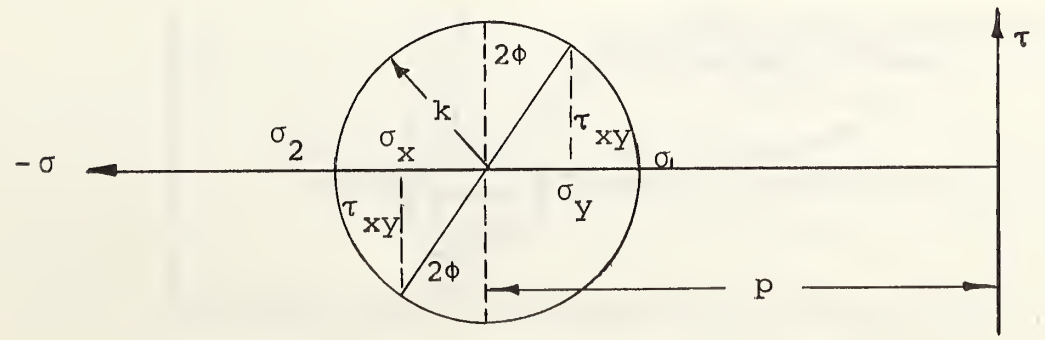

FIGURE 3 Mohr circle for the stresses at a point in a rigid-plastic solid showing p and ϕ.

These equations satisfy the yield criteria. "p" is the hydrostatic pressure as before, and $\phi + \frac{\pi}{4}$ is the anti-clockwise rotation between the positive x axis and the direction of the algebraically greatest principal stress.

The equilibrium equations now become:

$$\frac{-\partial p}{\partial x} - 2k \cos 2\phi \frac{\partial \phi}{\partial x} - 2k \sin 2\phi \frac{\partial \phi}{\partial y} = 0$$

$$\frac{-\partial p}{\partial y} - 2k \sin 2\phi \frac{\partial \phi}{\partial x} + 2k \cos 2\phi \frac{\partial \phi}{\partial y} = 0 \quad \text{.....(7)}$$

These are a pair of simultaneous quasi-linear partial differential equations. From the theory of partial differential equations,[13] it is easy to show that these equations are hyperbolic and that their characteristics have slopes

$$\frac{dy}{dx} = \tan \phi \quad \text{and} \quad \frac{dy}{dx} = \tan (\phi + \tfrac{\pi}{2}) \quad \text{.....(8)}$$

These characteristics, making angles of ϕ and $\phi + \frac{\pi}{2}$ with the positive x axis, are called α and β lines respectively. From a consideration of the Mohr circle in Figure 3, it is evident that the α and β lines coincide with the directions of maximum shearing stress.

The state of stress on an element is shown in Figure 4.

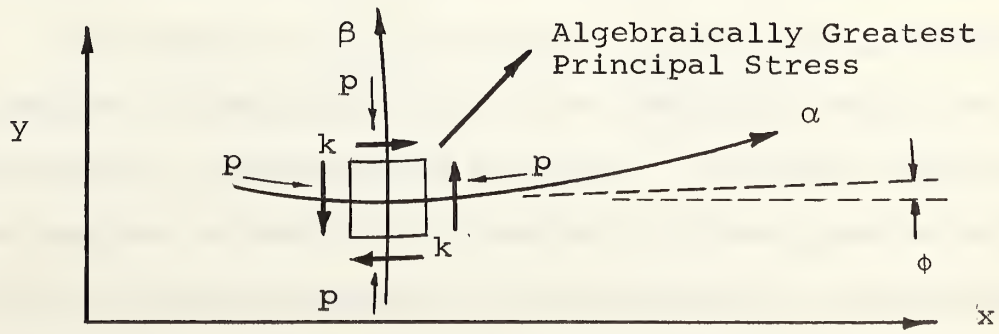

FIGURE 4 The state of stress of an element on an α and β line.

The relationships along the characteristics may be obtained by several procedures and may be expressed as

$$\begin{aligned} p + 2k\phi &= \text{a constant on an } \alpha \text{ line, and} \\ p - 2k\phi &= \text{a constant on a } \beta \text{ line,} \end{aligned} \qquad \text{.....(9)}$$

which are the Hencky equations.

The velocity equations for plane plastic flow are the continuity equation (eq. 4) and the isotropy equation.

$$-\cot 2\phi = \frac{\frac{\partial U_x}{\partial y} + \frac{\partial V_y}{\partial x}}{\frac{\partial U_x}{\partial x} - \frac{\partial V_y}{\partial y}} \qquad \text{.....(10)}$$

Equations (10) and (4) are a pair of simultaneous linear hyperbolic partial differential equations, and their characteristics coincide with those of the stress characteristics.

The relationships that hold along the characteristics may be found in terms of the velocity components referred to the x and y axes (that is U_x and V_y), but by expressing these relationships in terms of u, the velocity component along an α line,and v, the velocity component along a β line, the following equations first derived by Geiringer are obtained:

$$\begin{aligned} du - vd\phi &= 0 \text{ on an } \alpha \text{ line, and} \\ dv + ud\phi &= 0 \text{ on an } \beta \text{ line.} \end{aligned} \qquad \text{.....(11)}$$

The field of characteristics constitutes a solution to the problem of the plane flow in the deforming region of a rigid-plastic, non-hardening material. A further requirement for a complete solution to a problem in plane plastic strain is that the yield criterion is not violated in the non-deforming

region. A field of characteristics is known as a slip line field.

2.4. THE GEOMETRY OF THE SLIP LINE FIELD

Certain geometrical consequences follow for a curvilinear element formed between slip lines.

2.4.1 HENCKY'S FIRST THEOREM

"The angle between two slip lines of one family where they are cut by a slip line of the other family is constant along their length".

2.4.2 HENCKY'S SECOND THEOREM

If R is the radius of curvature of an α line and S is the radius of curvature of a β line, and s_α and s_β are the distances along the α and β lines respectively, then:

$$\frac{\partial R}{\partial s_\beta} = -1$$

$$\frac{\partial S}{\partial s_\alpha} = -1 \qquad \text{.....(12)}$$

or, the radii of curvature of the one family of slip lines change by the amount travelled along the other.

2.5 INDENTATION BY A SMOOTH WEDGE

The solution of the problem of indentation by a smooth wedge is given by Hill, Lee and Tupper[14] and is now outlined.

Consider the normal penetration of the surface of a semi-infinite block by a smooth wedge of semi angle θ as shown in Figure 5.

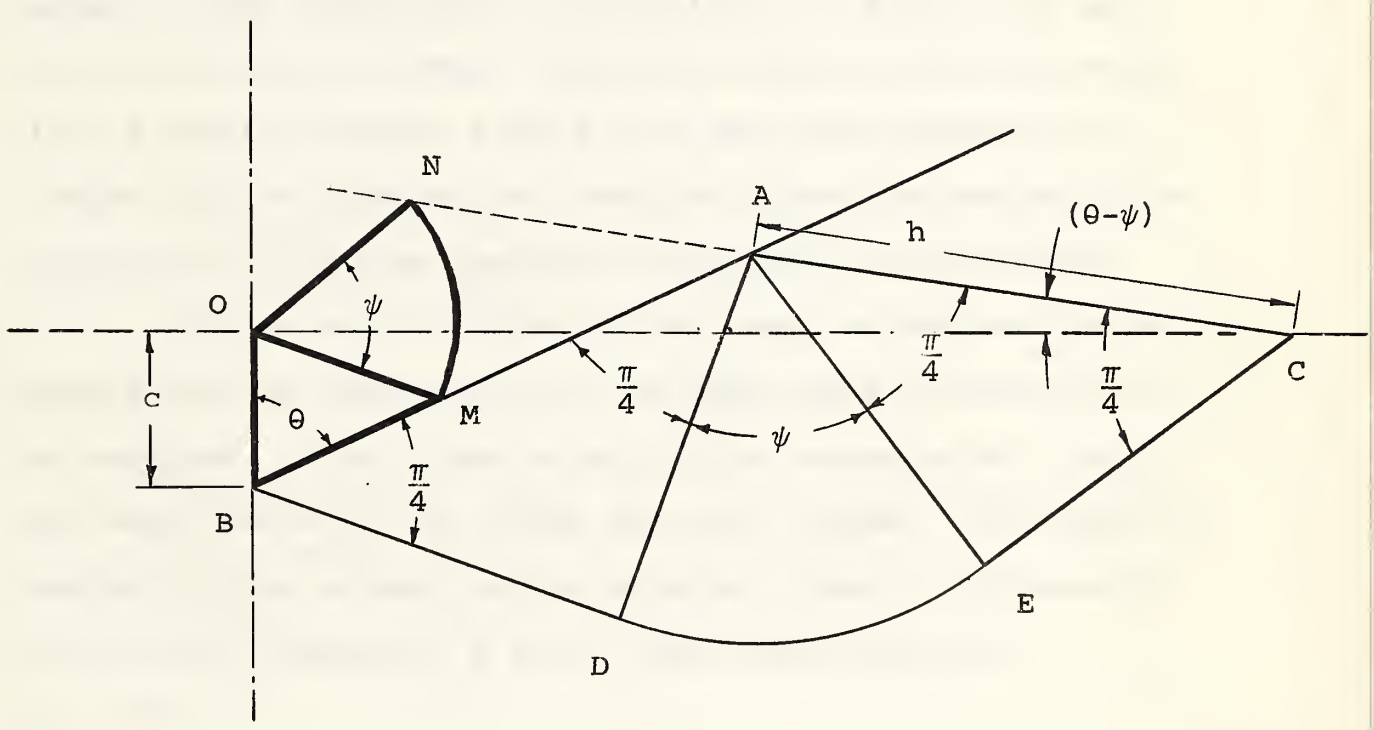

FIGURE 5 The indentation of a semi-infinite block by a smooth, frictionless wedge.

Region ABDEC is the plastically deforming region and line OC is the original undisturbed surface. The α and β lines in region AEC are straight lines which meet the surface AC at 45 degrees. AC is a principal stress plane for this region.

In region ABD the α and β lines are also straight and meet the surface BA at 45 degrees because surface AB has no tangential stress components acting on it. Point A is a stress singularity, and in region ADE, the α and β lines are arcs of circles, and straight lines, respectively. The depth of penetration of the tip of the wedge is c, and the length AB is represented by h.

In this (x,y) plane considered in Figure 5, the origin of the distortion is the point 0. If $\bar{r}$ is the position vector of an element from the origin of the distortion in the physical plane, and if c is made the characteristic length for the indentation, then the stress and velocity are functions of $\bar{r}/c$ when geometric similarity is preserved.

If the configuration at any stage of deformation is scaled down in the ratio c:1, the same shape of figure will be obtained. This figure in which the characteristic length has been made unity is called the unit diagram. The position vector $\bar{r}$ of an element in the physical plane is represented in the unit diagram by a point whose position vector is $\bar{\rho} = \bar{r}/c$.

The velocity of an element in space is*

$$\bar{v} = \frac{d\bar{r}}{dc} = \frac{d(\bar{\rho}c)}{dc} = \frac{d\bar{\rho}c}{dc} + \bar{\rho} \text{ , therefore, } \frac{cd\bar{\rho}}{dc} = \bar{v} - \bar{\rho} \quad \ldots(13)$$

All elements lying along the same radius describe the same trajectory in the unit diagram.

---

* See footnote in 1.3.4

The velocity diagram or hodograph for smooth wedge indentation is shown by the heavy lines in OBMN in Figure 5, and when this figure is transformed to the unit diagram, the condition that geometric similarity be preserved is that the projection of AB on the perpendicular to CAN be equal to the sum of the projections of BO and ON. This can be written:

$$\frac{h}{c} \cos \psi = \sin \theta + \cos (\theta - \psi) \quad \ldots\ldots\ldots\ldots\ldots (14)$$

The height of A above the original surface gives:

$$\frac{h}{c} \cos \theta - 1 = \frac{h}{c} \sin (\theta - \psi) \quad \ldots\ldots\ldots\ldots\ldots (15)$$

The elimination of h/c from (14) and (15) gives the relationship between θ and ψ.

$$\cos (2\theta - \psi) = \frac{\cos\psi}{1 + \sin \psi} \quad \ldots\ldots\ldots\ldots\ldots (16)$$

From the Hencky equations (9), it may be seen that the mean compressive stress in the region ABD is $k(1 + 2\psi)$, and the stress on surface AB consequently is

$$P = 2k (1 + \psi) \quad \ldots\ldots\ldots\ldots\ldots\ldots (17)$$

Considering a wedge of unit thickness, the load required to make the indentation is:

$$F' = 2P (h \sin\theta) = 4k (1 + \psi) h \sin \theta$$

In terms of c, this becomes:

$$F' = \frac{4k (1 + \psi) c \sin \theta}{\cos \theta - \sin (\theta - \psi)} \quad \ldots\ldots\ldots\ldots\ldots\ldots (18)$$

2.6 INDENTATION WITH A WEDGE SUBJECT TO FRICTION: THE LIMITING CASE

In 1953, Grunzweig, Longman and Petch[15] calculated the penetration, contact pressure and slip line field dimensions in plastic indentation, by using the Hill, Lee, and Tupper[4] theory applied to a rough wedge.

In this case, the angles BAD and DBA are no longer 45 degrees. (see Figure 6).

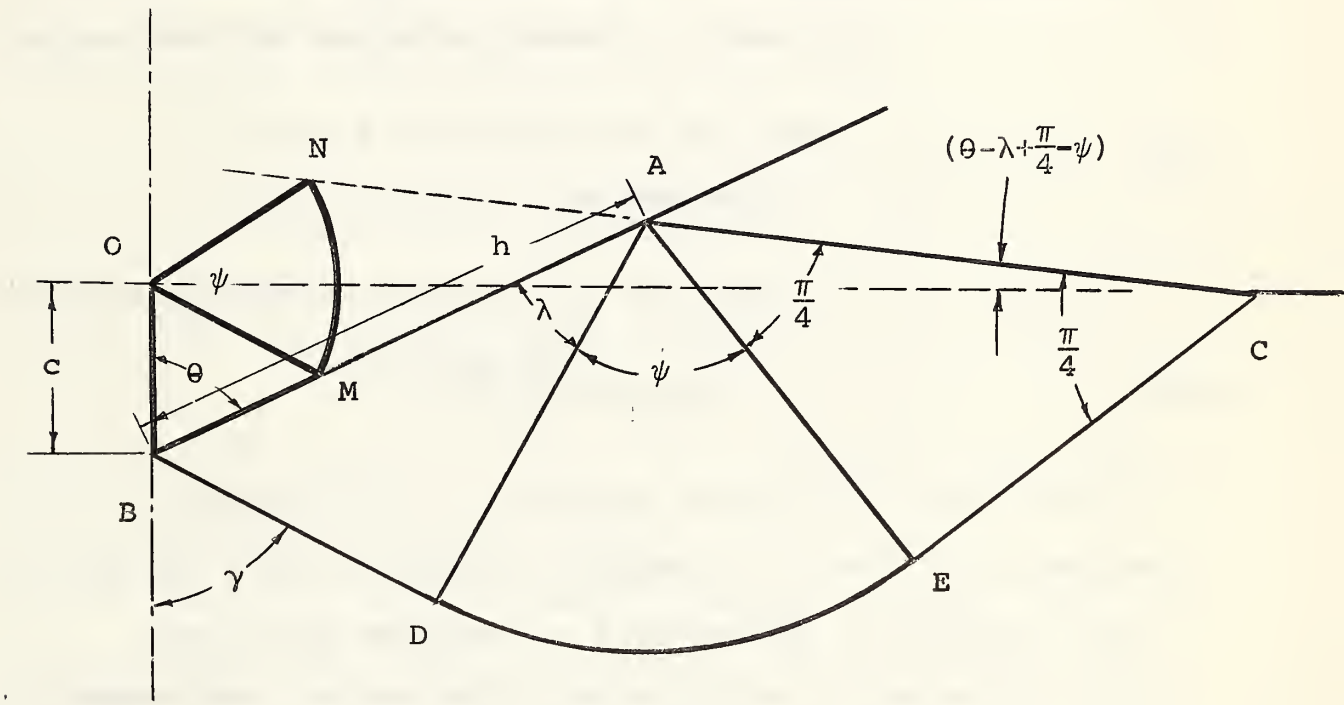

FIGURE 6 Plane strain wedge indentation with friction.

From Figure 6, the height of A above the original

surface is

$$h \cos \theta - c = \sqrt{2}\, h \cos \lambda \sin (\theta - \lambda + \frac{\pi}{4} - \psi) \quad \ldots\ldots (19)$$

The symbols used refer to 'geometry' analagous to the friction-less case. λ is angle BAD.

From the condition for continuing geometric similarity,

$$h \cos (\psi + \lambda - \frac{\pi}{4}) - c \cos (\theta + \frac{\pi}{4} - \psi - \lambda) = \frac{c \sin \theta}{\sqrt{2} \cos \lambda} \quad \ldots\ldots (20)$$

It can be shown by a consideration of the Mohr circle for the stresses in region ABD, that the normal compressive stress and the tangential shearing stress are:

$$P = k (1 + 2\psi + \sin 2\lambda), \text{ and}$$
$$\tau = k \cos 2\lambda, \text{ respectively.} \quad \ldots\ldots (21)$$

The coefficient of friction, μ, follows:

$$\mu = \frac{\cos 2\lambda}{1 + 2\psi + \sin 2\lambda} \quad \ldots\ldots (22)$$

Grunzweig et al calculate values of μ, h/c, P/k, λ, ψ, and ck/F' for 10 degree increments of $\theta = 0$ to 90 degrees.

For $\theta > 45$ degrees, as λ decreases, a limiting value is approached, beyond which the solution is not valid since the slip lines that pass through the point B (Figure 6) must meet at an angle greater than $\pi/2$. To show this, consider the tip of non-deforming metal at B which is acted on by stresses as shown in Figure 7 (a). The Mohr circle for the state of stress in this tip is shown in Figure 7 (b). Clearly the radius of this circle is greater than k unless $2\gamma \geq \frac{\pi}{2}$.

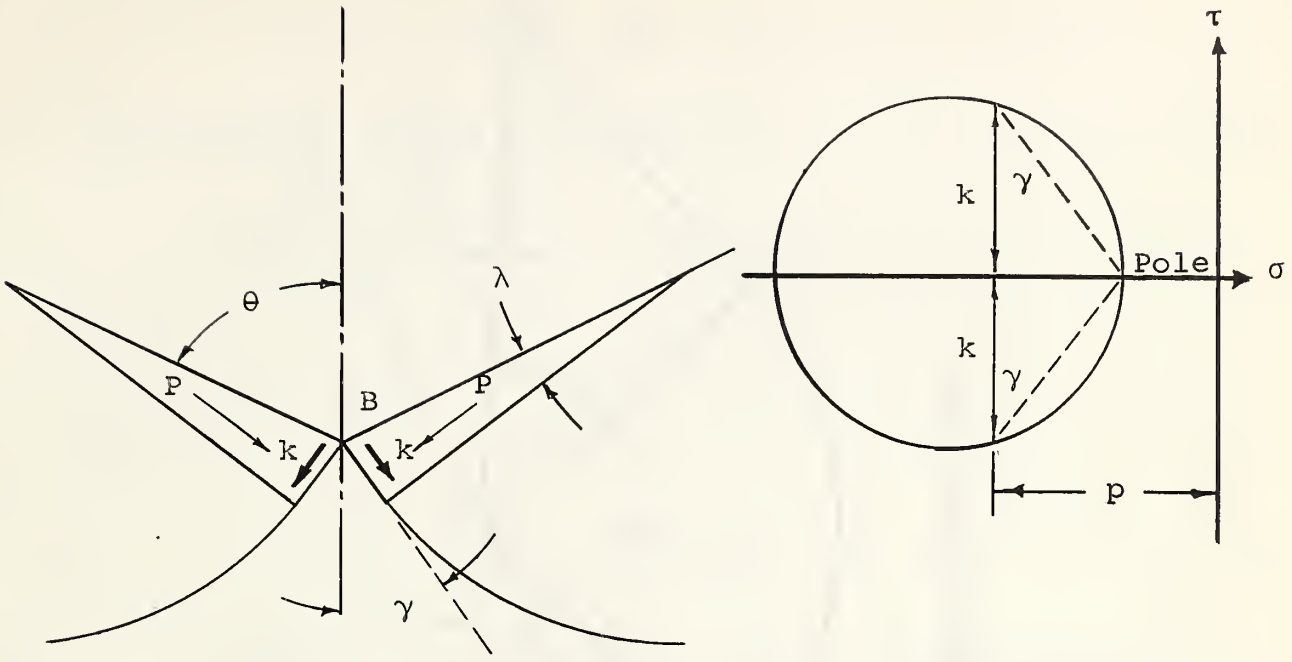

(a) (b)

FIGURE 7 Demonstration that there is a limiting value of λ and μ for the solution of Figure 6 when $\theta > 45^{\circ}$.

That is, the necessary condition for a statically admissible stress state just below B is $2\gamma \geqslant \frac{\pi}{2}$.

When $\theta > \frac{\pi}{4}$, and the wedge is perfectly rough, the solution requires a dead metal cap in contact with the wedge. Grunzweig et al, erroneously imply that for $\theta > \frac{\pi}{4}$, the limiting case of the solution indicated in Figure 6, with the slip lines at the wedge tip intersecting at right angles, gives the same values for indentation load, etc., as the solution that requires the dead metal cap shown in Figure 8.

For the dead metal cap solution, the condition that

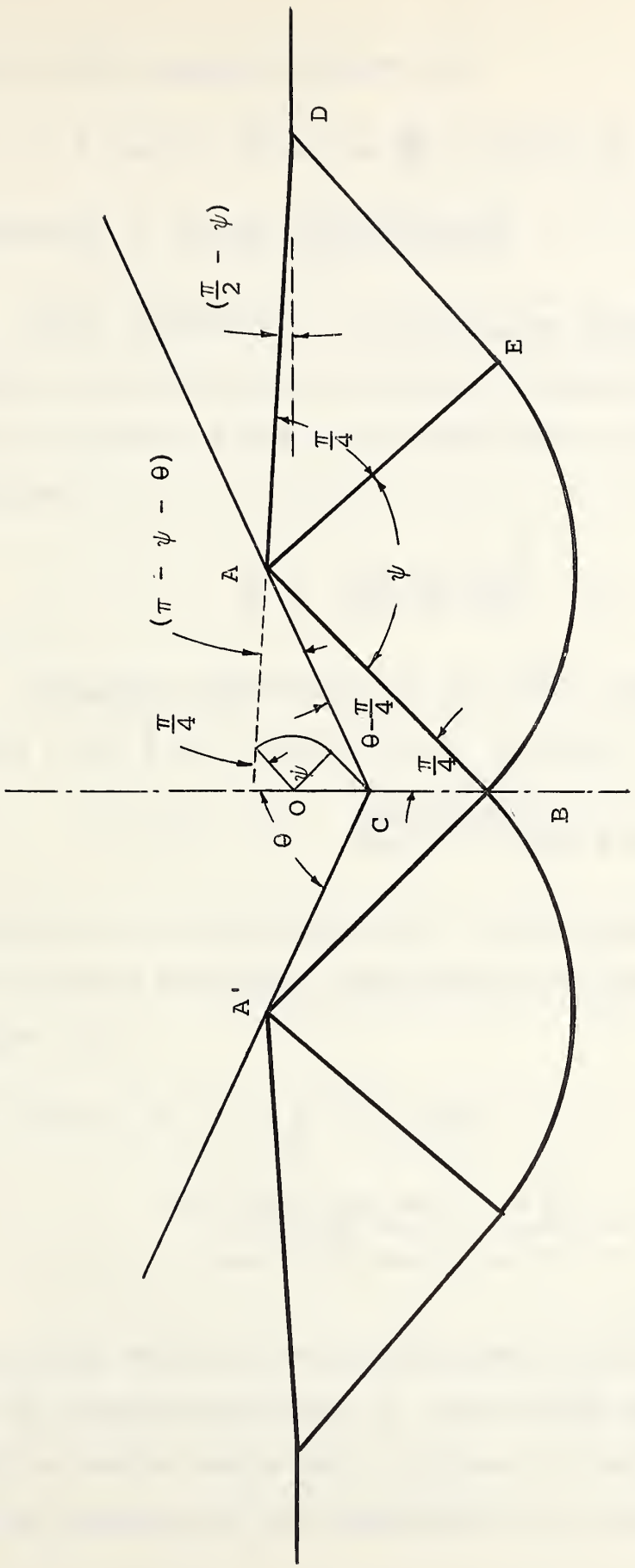

FIGURE 8 Correct Dead Metal Cap Solution for $\theta > 45$ Degrees

h = length AC

g = length AB

c = length OC

$\sqrt{2}g$ = length AD

D lies on the original surface is:

$$c = h \cos\theta - \sqrt{2}\, g \sin\left(\frac{\pi}{2} - \psi\right) \text{ but, } \frac{g}{\sqrt{2}} = h \sin\theta,$$

$$\text{therefore } \frac{h}{c} = \frac{1}{\cos\theta - 2 \sin\theta \cos\psi} \quad \ldots\ldots\ldots\ldots\ldots\ldots (23)$$

The condition for continuing geometric similarity is that the projection of CA on the perpendicular to AD is equal to the sum of the projections of CO and OH, from which condition:

$$\frac{h}{c} = \frac{\sin(\psi) + \frac{1}{2}}{\sin(\psi + \theta)} \quad \ldots\ldots\ldots\ldots\ldots\ldots (24)$$

Equating equations (23) and (24), the relationship between ψ and θ for the dead metal cap case is:

$$\sin(\psi) + \frac{1}{2} = \frac{\sin(\psi + \theta)}{\cos\theta - 2 \sin\theta \cos\psi} \quad \ldots\ldots\ldots\ldots (25)$$

Grunzweig et al eliminated h and c from equations (19) and (20) and called the resulting relationship the dead metal cap solution i.e.

$$\sin\theta + \sqrt{2} \cos\left(\theta - \psi + \frac{\pi}{4} - \lambda\right) \cos\lambda =$$

$$\frac{\sqrt{2} \cos\lambda \cos\left(\psi + \lambda - \frac{\pi}{4}\right)}{\cos\theta - \sqrt{2} \cos\lambda \sin\left(\theta - \psi + \frac{\pi}{4} - \lambda\right)} \quad \ldots\ldots (26)$$

The critical value of the coefficient of friction can be found by considering Figure 9, which shows the state of stress acting on region ABC shown in Figure 8. This value can be found by considering the extension of the statically admissible

solution into the dead metal cap.

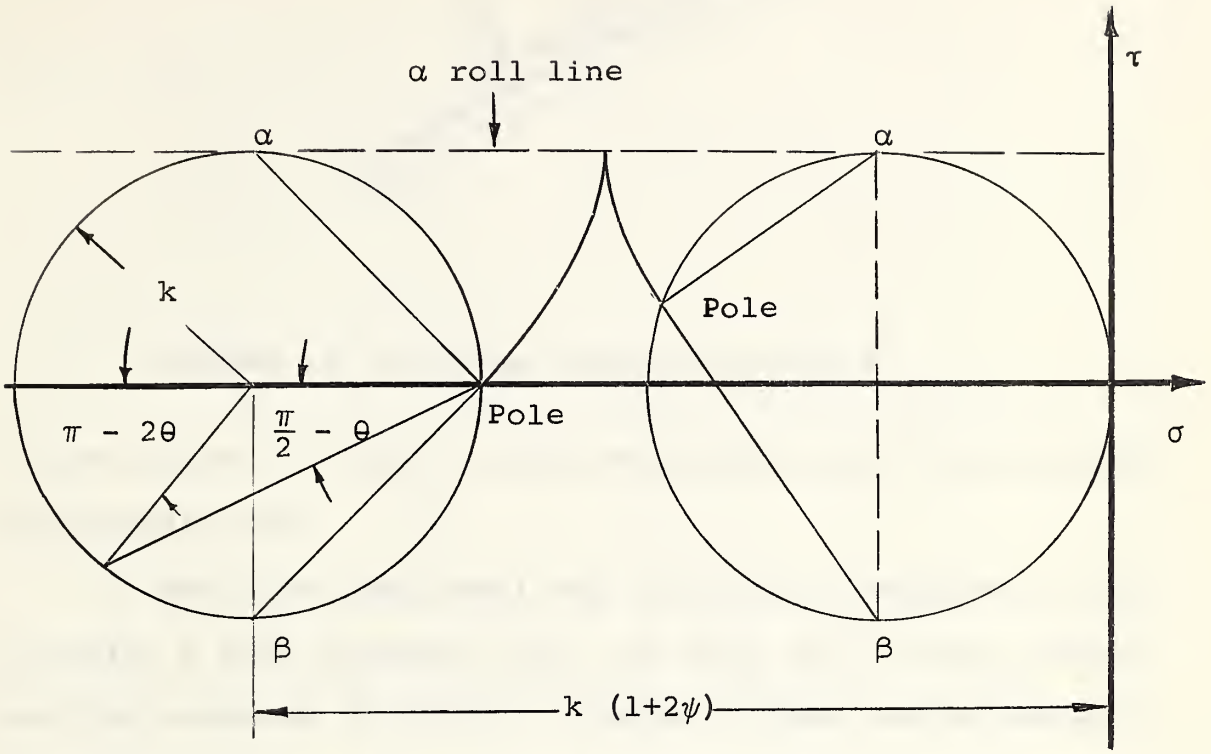

FIGURE 9 Stress plane for indentation with perfectly rough wedge with $\theta > 45^\circ$

The circle with center (-k,0) and radius k represents the stress state in area ADE. A circle in the (σ,τ) plane with center $(-k(1 + 2\psi),0)$ and of radius k represents the state of stress in area CBA.

It can be seen that the stresses shown in Figure 10 act on plane AC. It follows, then that the coefficient of friction on the wedge must satisfy the inequality:

$$\mu \geqslant \frac{\sin 2\theta}{1 + 2\psi - \cos 2\theta} \quad \ldots\ldots\ldots\ldots\ldots\ldots (27)$$

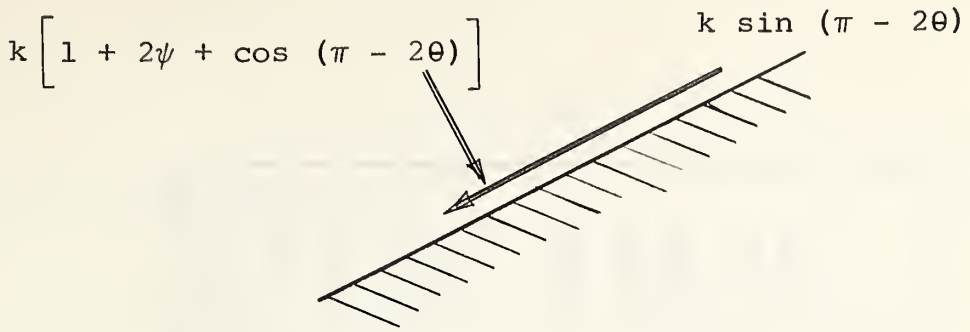

FIGURE 10 Stresses acting on plane AC.

if the state of stress in the dead metal cap is to be statically admissible.

The true dead metal cap solution is obtained by calculating μ from equation (27), h/c from (23) or (24) and by solving equation (25) for ψ. Table I gives the values obtained for the dead metal cap solution and for the limiting case of the solution of Figure 6 with $\gamma = \pi/4$, for θ = 50, 60, 65, 70, 80, and 90 degrees. The column ck/ F' for the true dead metal cap case is calculated from the equation:

$$\frac{ck}{F'} = \frac{\cos(\theta) - 2\sin\theta\cos\psi}{2\left[\left((1 + 2\psi) - \cos 2\theta\right)\sin\theta + \sin 2\theta\cos\theta\right]} \quad \ldots\ldots(28)$$

where F' = the load per unit width of the wedge.

There is an anomaly here. It would appear that for a specified load and material, the dead metal cap solution gives a deeper indentation than the other solution proposed by Grunzweig et al. Further investigation in the range of the

TABLE I

PARAMETERS FOR WEDGE INDENTATION

θ	μ	h/c	P/k	λ	ψ	ck/ F'
50	*.242	2.11	4.08	5°	83°10'	.0626
	+.240	2.07	4.10		83°57.5'	.0637
60	*.195	2.78	4.44	15°	84°07'	.0421
	+.193	2.67	4.50		85°51.4'	.0433
65	* Not calculated.					
	+.164	3.16	4.67		86°39.4'	.0348
70	*.135	4.16	4.75	25°	85°27'	.0256
	+.133	3.90	4.82		87°23.5'	.0270
80	*.069	8.41	4.99	35°	87°18'	.0120
	+.068	7.68	5.04		88°44.2'	.0130
90	0.0	∞	5.14	45°	90°00'	-----

* Solution of Figure 6 with $\gamma = \frac{\pi}{4}$.

\+ Dead metal cap solution.

critical value of the coefficient of friction would be desirable.

2.8 THE KNOOP TEST

The form of the indentation produced by a Knoop indenter is shown in Figure 11. This is the indentation in a theoretical rigid-plastic solid.

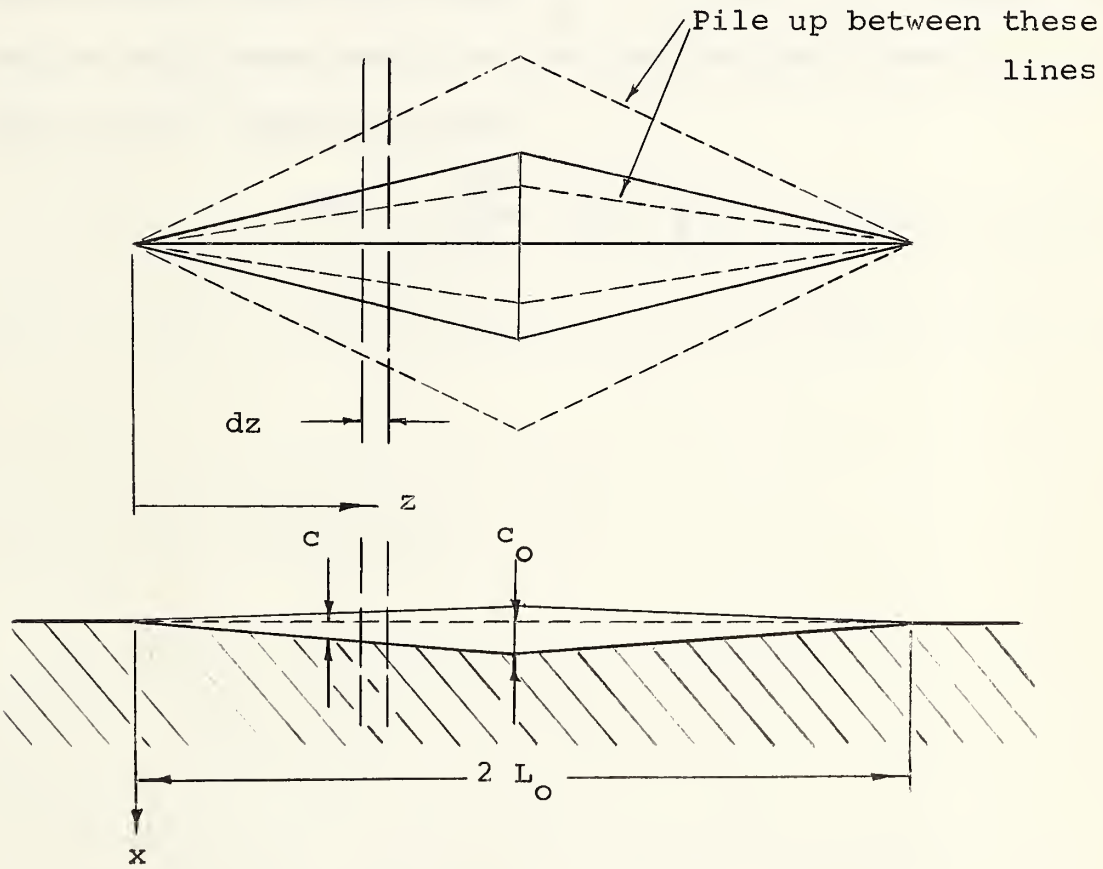

FIGURE 11 The Knoop Indentation

The depth, c, at any distance z from the end of the indentation is:

$$c = \frac{c_o z}{L_o} \quad \text{.....(29)}$$

Considering each element of the indentation as a problem in plane strain wedge indentation, and letting $ck/F' = Q$ (values of Q are given in Table I), then, F', the load per unit width becomes:

$$F' = \frac{ck}{Q} = \frac{c_o kz}{L_o Q} \quad \ldots\ldots\ldots\ldots\ldots\ldots\ldots\ldots (30)$$

By integrating this expression over the entire length of the indentation, and noting that $c_o = L_o \cot\left(\frac{\eta}{2}\right)$, where η is the included Knoop angle in the longitudinal direction, the total load F, may be written:

$$F = \frac{L_o^2 k}{Q} \cot\left(\frac{\eta}{2}\right) \quad \ldots\ldots\ldots\ldots\ldots\ldots\ldots\ldots (31)$$

CHAPTER 3

THE COMPRESSION STRESS STRAIN CURVES

In order to evaluate the yield stress in pure shear, k, it is the most convenient to evaluate Y, the uniaxial yield stress, and to then obtain k from the relationships $k = Y/2$ or $k = Y/\sqrt{3}$, depending on which of the two yield criteria is accepted. In a tensile test, the specimen necks at a relatively low strain. Consequently for large strains a compression test is usually used to obtain a uniaxial stress strain curve.

3.1 THE TAYLOR METHOD

Taylor[16] has shown that the stress-natural strain curves for most metals, obtained in tensile and compressive tests, coincide over the range of validity of the tensile test, and has described a method for obtaining the stress-natural strain curve for large strains.

Taylor's method was used to obtain stress strain curves for the metals used in these tests and is as follows. A cylinder of initial height diameter ratio of about unity is compressed by increments of loading between lapped lubricated dies. After each increment of compression, the cylinder is

removed and the height measured. Before any significant barreling occurs, the diameter is reduced by turning. This procedure is repeated until the desired natural strain is obtained.

3.2 THE COOK AND LARKE METHOD

Cook and Larke[17] have shown that curves of true resistance to homogeneous deformation may be obtained by compressing as few as four cylinders and analysing the resulting curves.

The continuous compression curves of nominal stress against percent height reduction for initial diameter to height (d_o/h_o) ratios are of 0.5, 1.0, 2.0 and 3.0 are plotted as shown in Figure 12 (a). The nominal stress is defined as the load multiplied by the current height and divided by the volume of the cylinder. The curve of nominal stress against the (d_o/h_o) ratios is plotted for a given reduction as shown in Figure 12 (b), and the curve extrapolated to $d_o/h_o = 0$ gives the compressive stress necessary to produce the reduction independently of frictional effects. Figure 12 (c) follows.

Ford[18] found that with specimens of equal initial diameters, it was simpler and more accurate to extrapolate on the basis of equal loadings instead of equal percentage reductions. In this modification, the incremental loading technique can be used, so no allowance for elastic strains in the apparatus is necessary. Ford suggested relubrication between the increments.

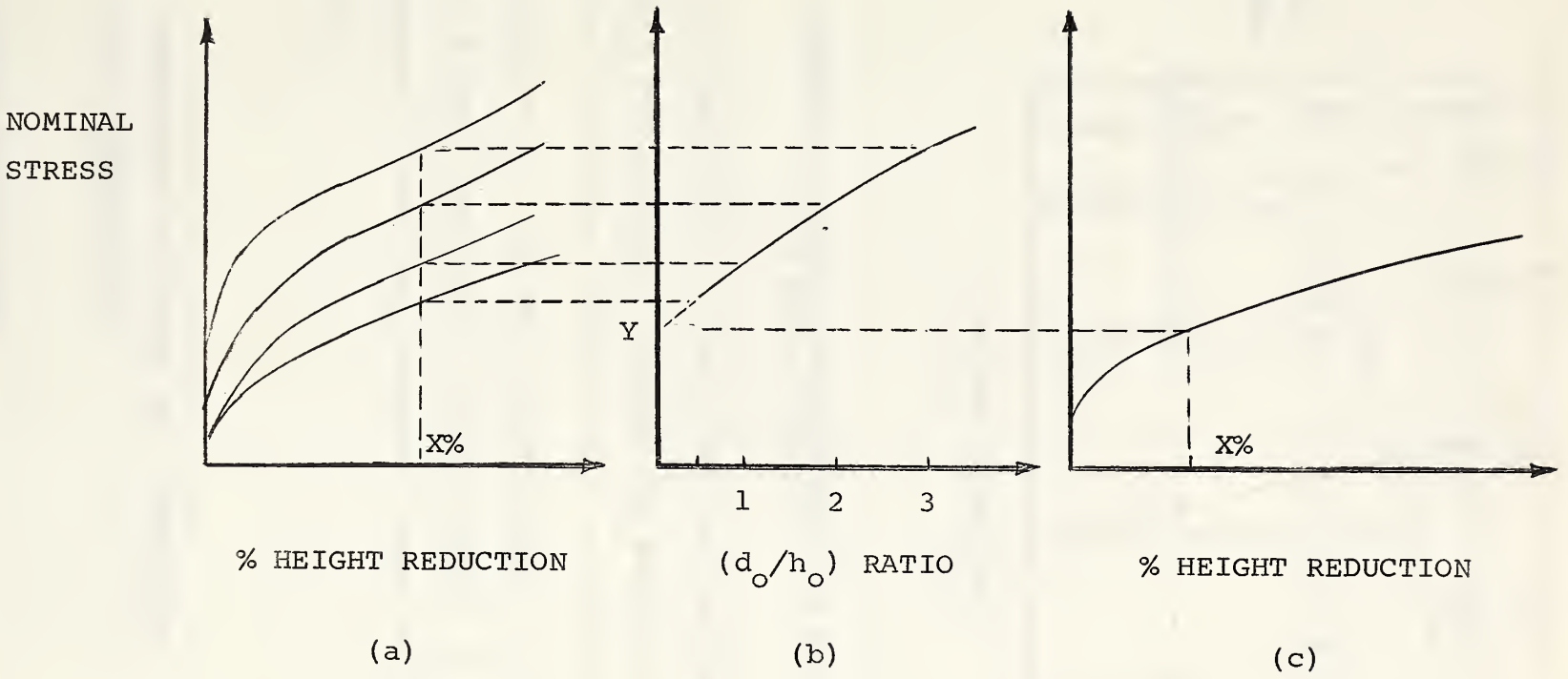

FIGURE 12 Stress-strain curve by the Cook and Larke Analysis

The principle is illustrated in Figure 13.

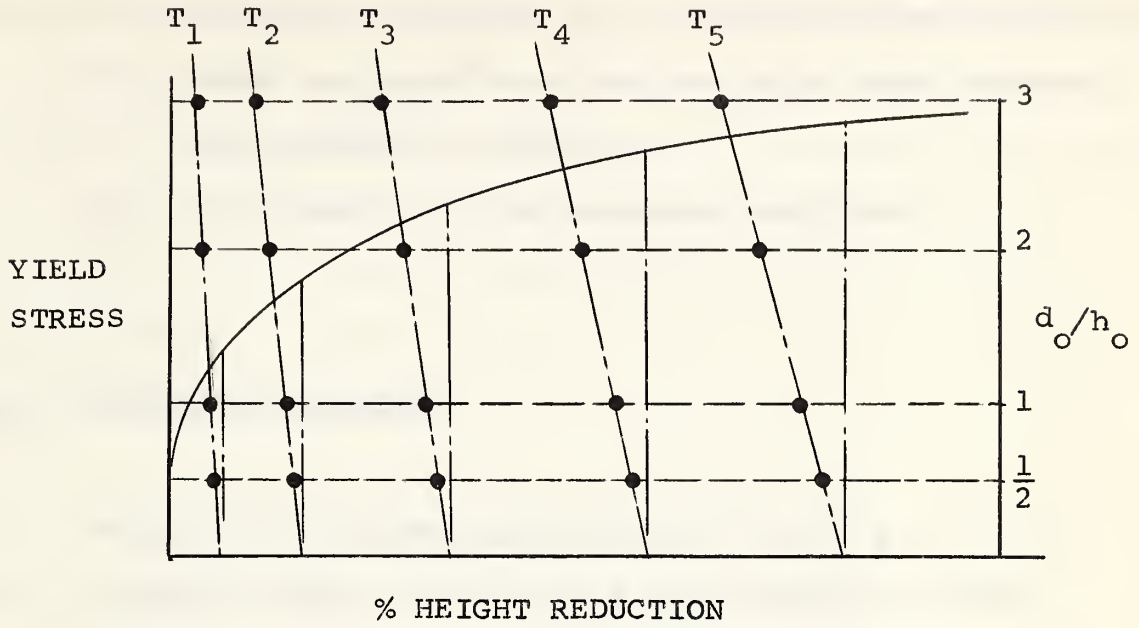

FIGURE 13 Ford's modification of the Cook and Larke Method.

Extrapolation of the curve (not necessarily a straight line) for a given load, T, gives the percent reduction in height that would have occured with an infinitely long test piece ($d_o/h_o = 0$). For any gauge length, h_o, in the infinitely long test piece, the ideal current height, h, can be found, and consequently the ideal current cross sectional area and true stress.

3.3 COMPRESSION CYLINDER AND IDENTATION BLOCK PREPARATION

3.3.1 METALS INVESTIGATED

The following metals were used for the indentation

experiments:

(1) superpure aluminum (in two heat treated conditions).

(2) 0.06% tellurium lead (in the fully work hardened and annealed conditions).

(3) mild steel (in the annealed condition).

3.3.2 SUPERPURE ALUMINUM

Blocks, the largest of which was 2 1/2" x 2 1/2" x 1 1/2", were cut from a fifty pound ingot number 56075Q06 supplied by the Aluminum Company of Canada Limited. These were successively deformed by a fifty percent reduction in three orthogonal directions, and then placed in the annealing furnace. The furnace was brought up to 570 degrees F, held there for seven minutes, and then the blocks were air quenched and specimens were machined from them. This is heat treatment 1.

Another set of aluminum blocks was cut from the same ingot, deformed in the same manner and placed in the annealing furnace. The furnace was brought up to 650 degrees F, turned off and allowed to cool down for four hours to 300 degrees F, after which the blocks were taken out, air cooled, and the specimens machined from them.

3.3.3 0.06% TELLURIUM LEAD (WORK HARDENED)

The lead was supplied in billets 4" x 4" x 12".

Blocks were cut from the billets and reduced forty percent in three orthogonal directions. This was done to minimize the development of anisotropy. Several of the blocks developed visible fissures while in compression. These were rejected.

Specimens were machined and to prevent possible annealing at room temperature, they were kept between thirty and forty degrees F until used.

3.3.4 0.06% TELLURIUM LEAD (ANNEALED)

The blocks were prepared in the same manner and then annealed for 1 1/2 hours at 220 degrees C. The specimens were then machined to size.

3.3.5 MILD STEEL

Mild steel, supplied in 1 1/2 inch diameter bar stock, was brought up to 1600 degrees F, held there for 1/2 hour, and then cooled in the furnace (one day). Specimens were then machined from the stock.

3.3.6 COMPRESSION TEST SPECIMEN PREPARATION

All cylinders were turned on a lathe and the ends were parallel to within 0.001 inches. Between successive

stages of bulging, in the Taylor method, the cylinders were turned down as shown in Figure 14. A small disc with a countersunk hole for a live center on one side and a smooth side towards the specimen provided lateral support. The driving torque from the headstock goes through a section of bar stock steel which is slightly roughened on its surface of contact with the specimen.

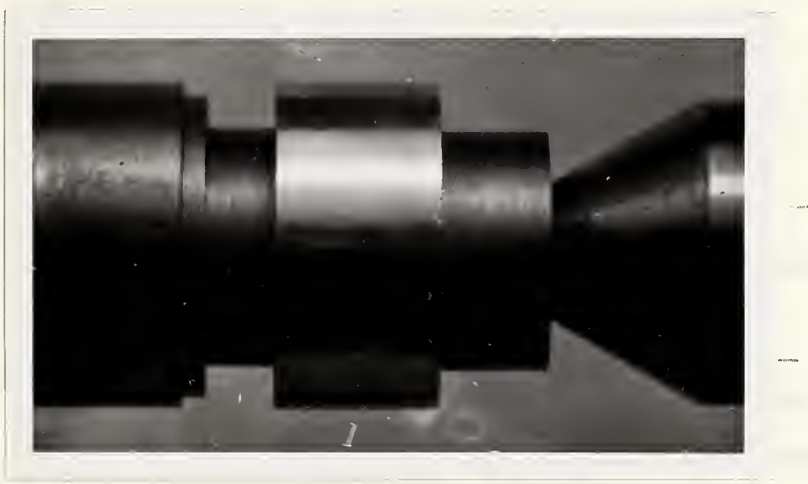

FIGURE 14 Turning down the test cylinders

3.4 COMPRESSION TEST APPARATUS AND PROCEDURE

The prepared cylinders were accurately measured before compression. For the procedure outlined by Taylor, vaseline was used as a lubricant for the aluminum and lead, while calcium oleate was used for the steel. Some difficulty occured with the calcium oleate; when an excess of this lubricant

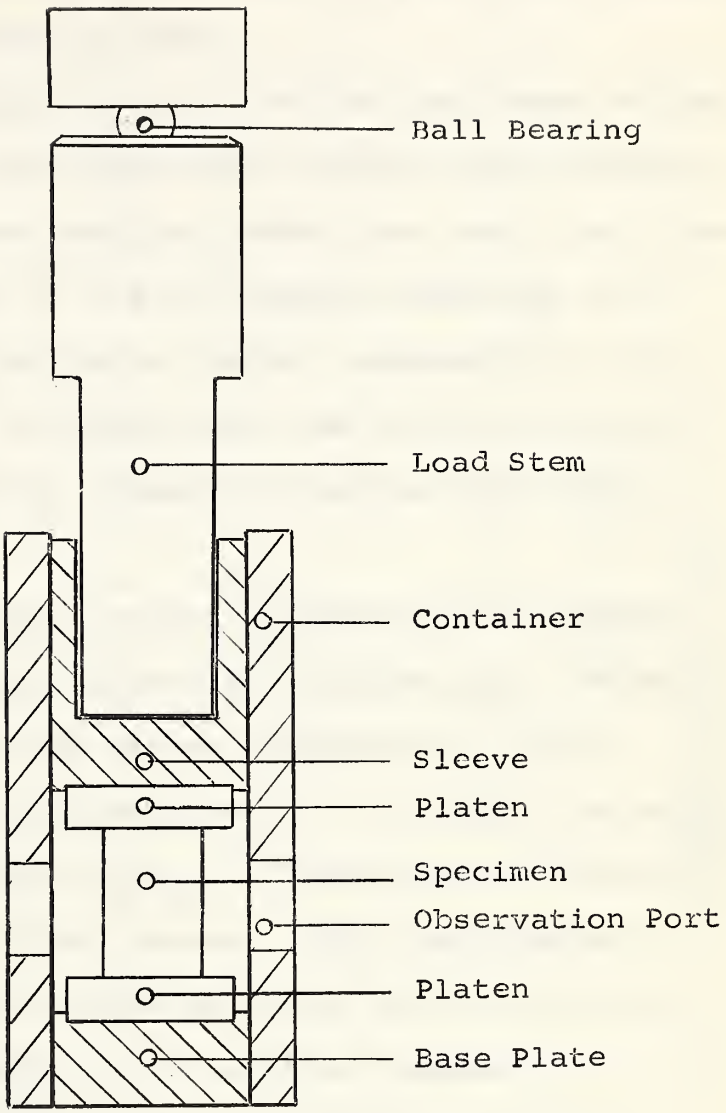

FIGURE 15 The compression sub-press

($\frac{1}{2}$ size)

was used, the ends of the specimen became noticably concave. This difficulty was overcome by using minute amounts of lubricant. When too much vaseline was used, it pitted the surface of the specimen, especially the lead.

For the Ford modification of the Cook and Larke method, the increments of load were larger than for the Taylor method. For the steel, lubrication (calcium oleate) was used, but since the results obtained with it did not compare favorably with the results obtained by the Taylor method, especially at low strains, (see Figure 18) no lubrication was used in obtaining the Cook and Larke curve for annealed tellurium lead shown in Figure 16.

The compression tests on the aluminum and work hardened lead using the four cylinders with varying d_o/h_o ratios were unsuccessful because the taller cylinders (2" high) showed inhomogeneity in their deformation. It should be noted that the steel cylinder with $d_o/h_o = 1/2$ exhibited a form of plastic buckling at the higher strains. This buckling may have been initiated by one of the principal axes of plastic anisotropy being at an angle to the axis of compression.

The compression test curves for aluminum, lead and steel are shown in Figures 16, 17, and 18.

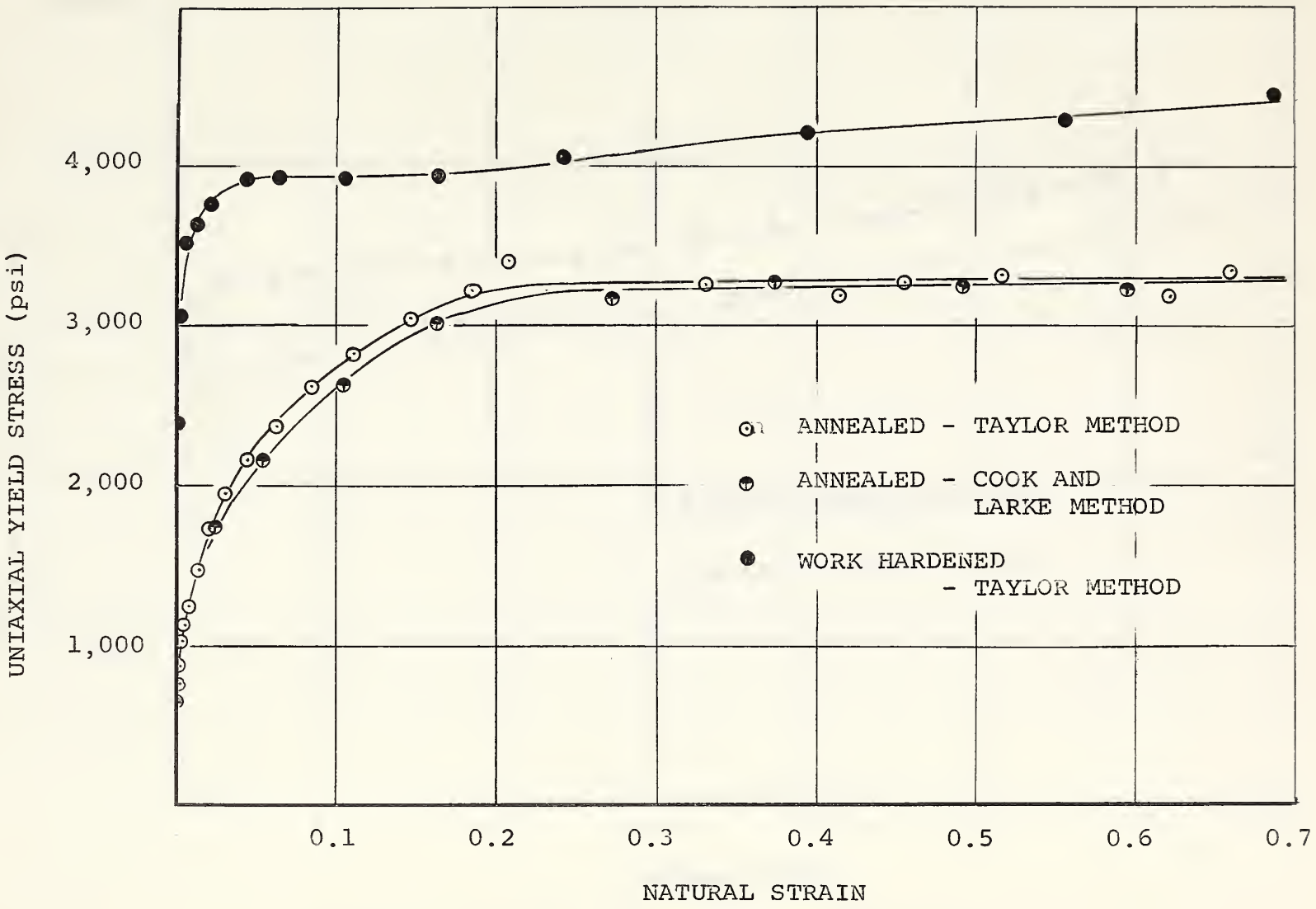

FIGURE 16 Stress natural strain curves for 0.06% tellurium lead

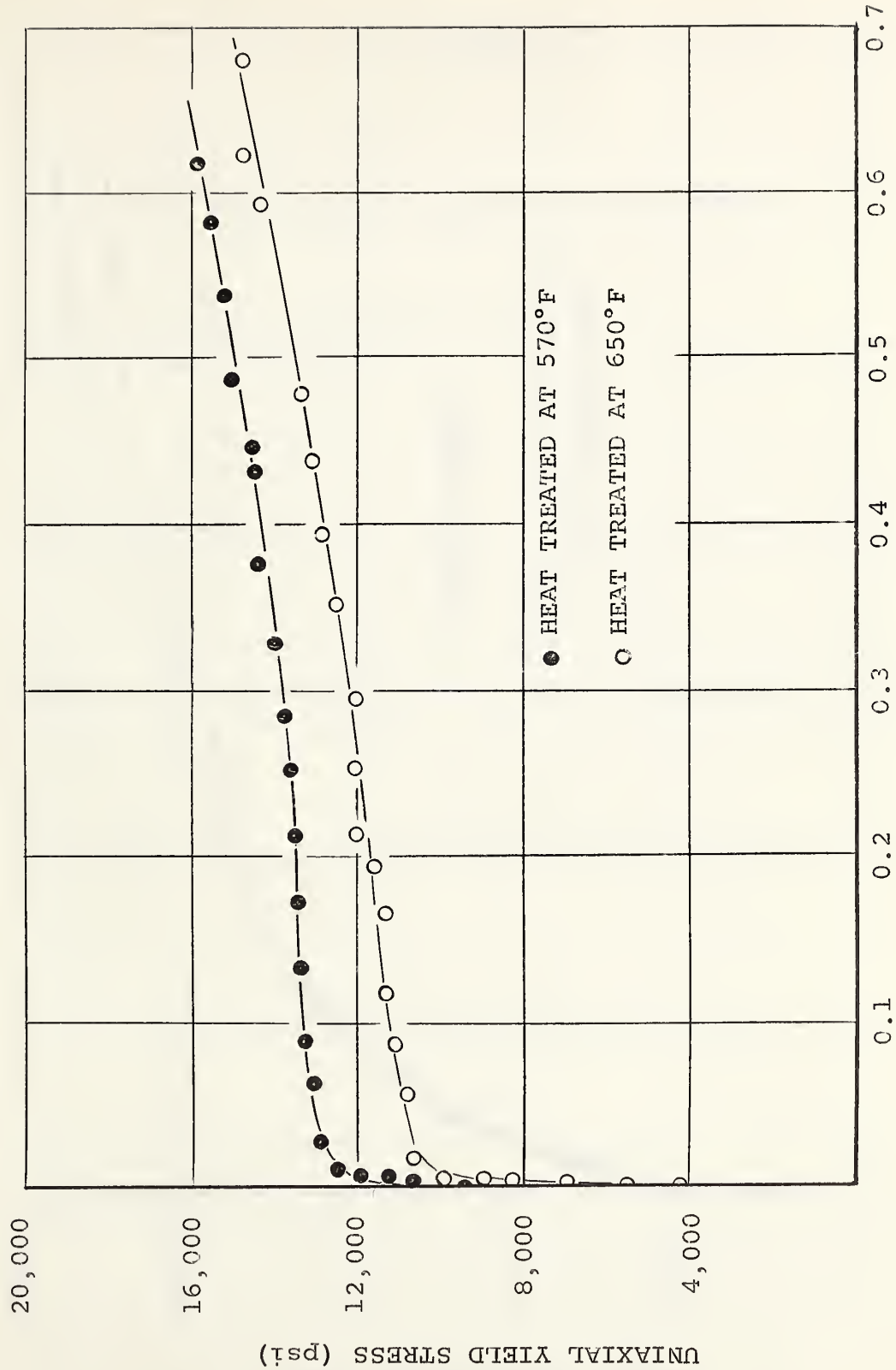

FIGURE 17 Stress natural strain curve for superpure aluminum

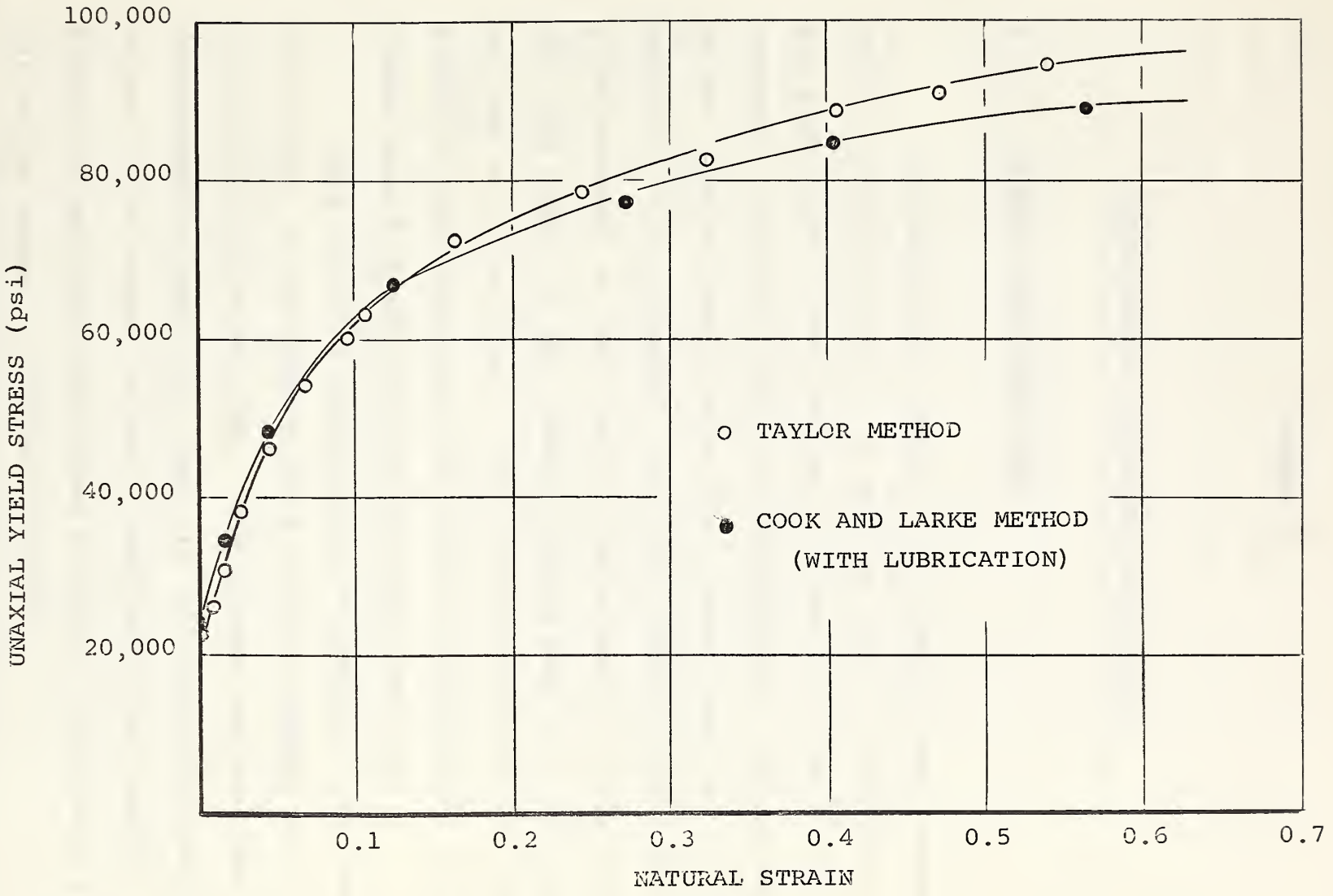

FIGURE 18 Stress natural strain curve for 0.20% carbon mild steel

CHAPTER 4

EXPERIMENTAL PROCEDURE AND RESULTS

4.1 GENERAL CONSIDERATIONS

For meaningful results, the indenter must possess certain characteristics. It must be large in comparison with the grain size of the specimen if there is to be continuing geometric similarity during the indentation. The hardness of the indenter should be at least three times that of the materials to be indented[19], and the indenter should have a rigid mounting so that elastic displacement is minimized. The four planes of the indenter should meet at a point and not form a "chisel edge". The surface finish of the indenter should be very smooth and the lines of intersection of the planes should be well defined and free from nicks.

On a two inch diameter bar of Keewatin tool steel, the four planes of the indenter were milled by making use of the calculated strikes and dips. The optimum included apex angles recommended by Knoop (130° and 172° 30') were obtained accurate to the nearest minute. The stem of the indenter (see Figure 19) was then turned down so that it would have a close fit in the sleeve of the test sub-press.

The indenter was hardened by placing it in a furnace,

raising the temperature to 1640 degrees F, holding for twelve minutes, and then quenching the indenter in oil. The Vickers hardness was then about 900 as compared with 246 before hardening. Both readings were taken with 1,000 gm loads and a ten second dwell on a Durimet Micro-Hardness Tester. Rough lapping of the surfaces to remove the slight scale formed during the hardening process preceeded measurement of the included angles which were then 172° 30' and 130° 19'. As well as a variation from the ideal Knoop angles, a "rounding off" of the intersections of the planes was noted.

The working surfaces were then ground on a surface grinder but the accuracies of the angular settings on the available grinder prevented close angular tolerances from being achieved. Careful hand lapping and polishing produced sharply defined plane intersections and a smooth finish with apex angles of 172° 06' and 129° 48' as shown in Figure 19. All angular measurements were made on a Leitz measuring microscope.

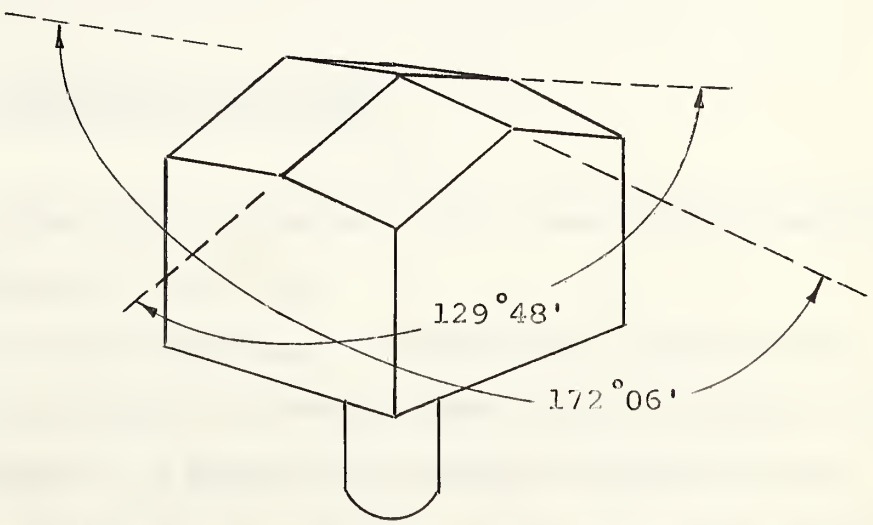

FIGURE 19 Hardened Keewatin Tool Steel Knoop Indenter (Approximately Full Size)

Knoop et al[20] found that indenters with included angles from 126° to 136° in the transverse direction and 170° 44' to 173° 52' in the longitudinal direction gave essentially the same hardness number when the calculations were based on the individual indenter's "unrecovered area". The hardness numbers determined by the use of this steel indenter are, therefore, computed on the actual geometry shown in Figure 19.

With the optimum included apex angles, the Knoop hardness can be found from the relationship

$$H_k = \frac{2F}{(2L_o)^2 \tan 65^\circ \cot 86^\circ 15'} \quad \text{.....(32)}$$

where:

H_k = Knoop hardness number (kg/mm^2)

F = Load on the indenter (kg)

$2L_o$ = Length of the long Knoop diagonal (mm)

4.2 THE INDENTATION SUB-PRESS

The indentation sub-press with a specimen in position is shown in Figures 20 and 21.

Since it was necessary to remove the specimen from the indenting sub-press for measurement of the diagonals after each load increment, a means of accurately re-positioning the specimen and indenter was needed. For re-positioning the

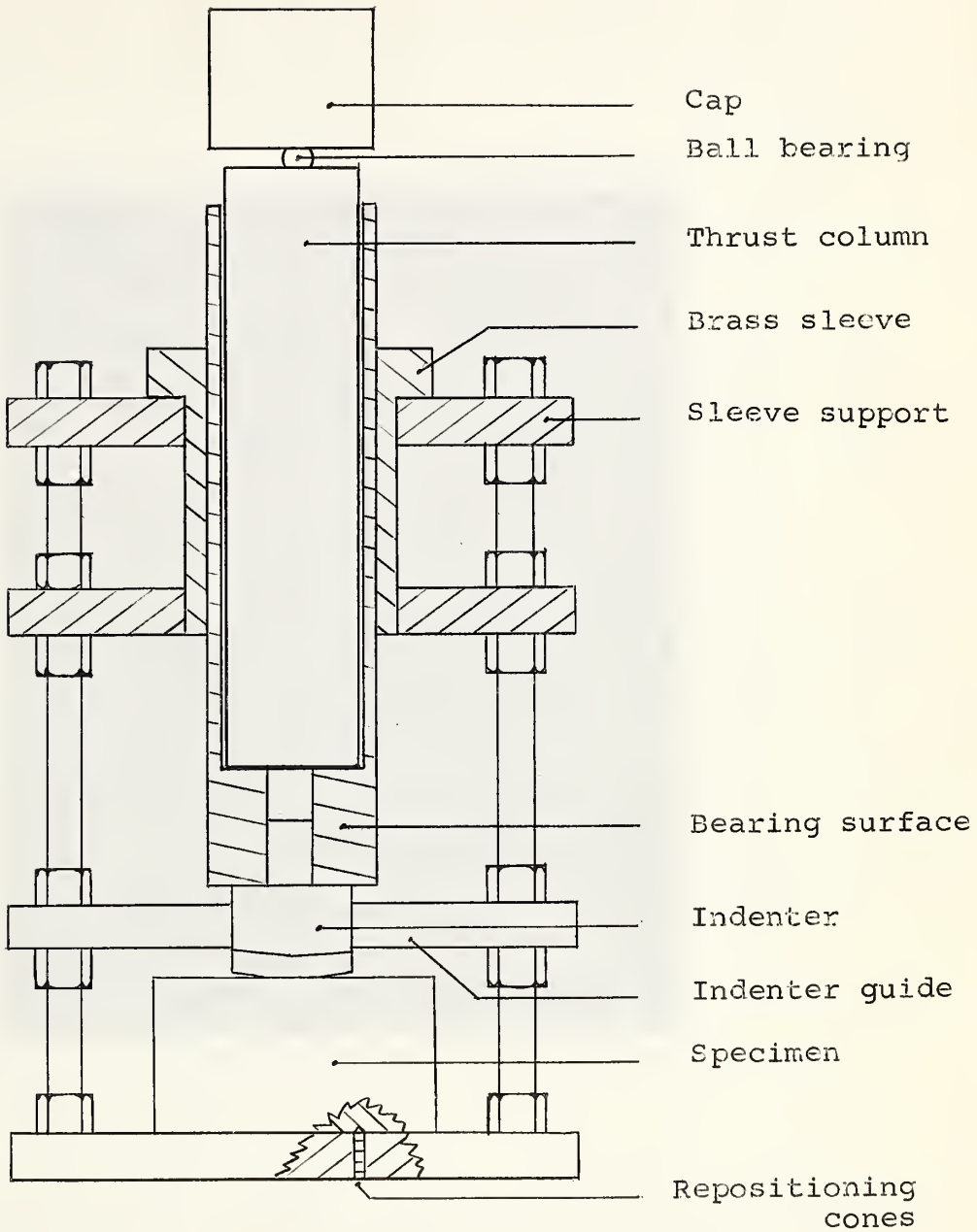

FIGURE 20 Indentation sub-press (1/2 scale)

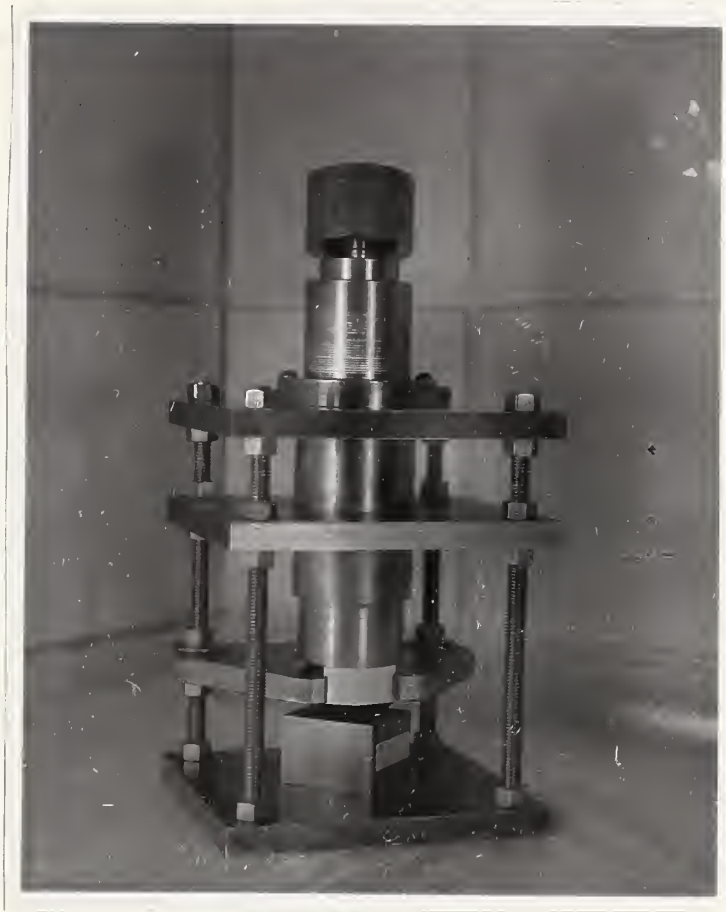

FIGURE 21 Indentation Sub-Press

specimen, three hardened small steel cones were set in the bottom plate and projected about one sixteenth of an inch above the surface (see Figure 22). Before indenting began, the test specimens were pressed upon these cones until the bottom of the specimen was flush with the plate. (In some cases, it was necessary to file away the specimen pile up around the cones before the specimen would seat properly). During this process the surface of the specimen was protected by several layers of paper tissue. The necessary force was transmitted from the bearing surface (see Figure 20) through a 1/2 inch thick steel plate to the specimen. Care was taken not to yield the specimens during this procedure.

For re-positioning the indenter, a removable plate attached to two of the four columns restricted the indenter from rotating but left it free to travel in a vertical direction (see Figure 22). To insure a consistant placement of the indenter in the slot, one side of the indenter was marked.

The alignment of the indenter's axis with the axis of the sub-press was checked by considering the longer diagonal of the indentation. Measurement of the indentations formed by various loads showed that one portion of the diagonal, which was measured from the extremity, to its point of intersection with the shorter diagonal, was 0.02 inches longer than the other portion. Thibault and Nyquist[21] investigated the effect of assymmetry on the Knoop numbers and found that if the length of the shorter portion of the long diagonal was

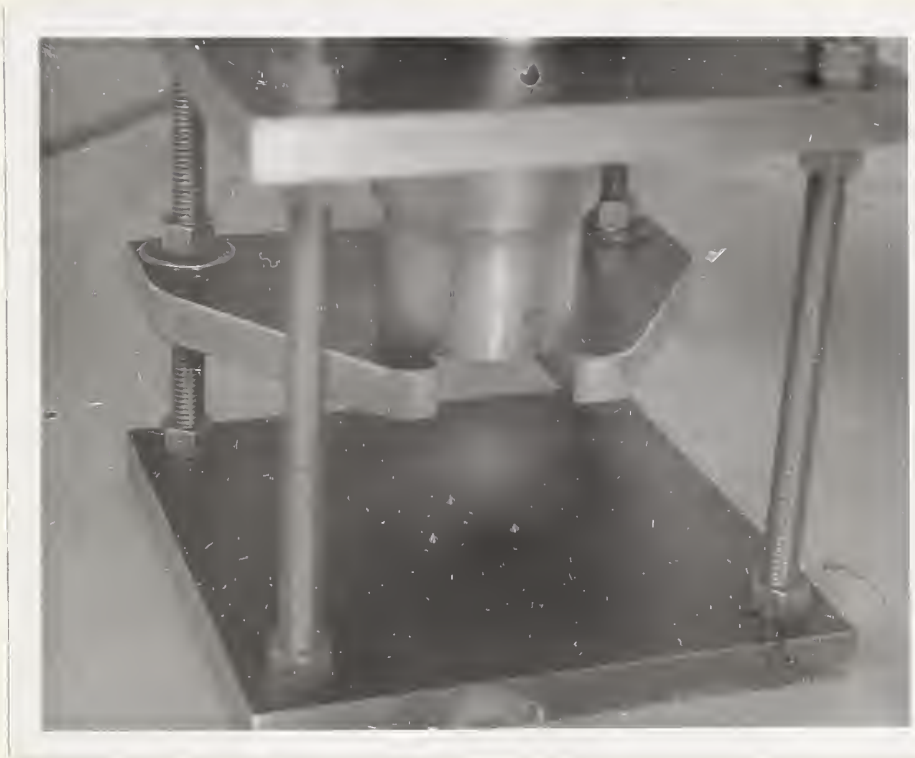

FIGURE 22 Indentation Sub-Press showing method of re-positioning specimen and indenter.

at least 80% of the length of the longer portion, virtually no lowering of the Knoop number occurred. For this reason, only indentations with total diagonal length greater than 0.20 inches are accepted as reliable.

4.3 SPECIMEN PREPARATION

All specimens were prepared at the same time and in the same manner as their corresponding compression test cylinders. The faces were parallel to within .001 inch and the surfaces to be indented were carefully finished by a shaper. Only the steel specimens were further prepared by lapping.

With the exception of the steel cylinders which were 1 1/2 inches in diameter, the specimens were blocks with a prepared surface approximately 2 inches x 2 inches, and a depth never less than 7/8 of an inch and usually greater than 1 1/4 inches.

Hill[22] investigated the theoretically critical specimen size for the plane strain problem of wedge indentation. Considering the possible depth to which this Knoop indenter could penetrate, a conservative estimate for the minimum specimen thickness is 0.8 inches. This is the minimum thickness necessary to prevent the plastic region from extending to the bottom of the specimen. Hill notes that the critical depth for the actual three dimensional case is somewhat less than for plane strain wedge indentation.

The width of specimen necessary to prevent permanent lateral deformation is conservatively estimated to be five times the width of the impression. In all cases the actual specimen width was greater than eight times the width of the indentation.

As a check on lateral plastic deformation of a specimen, an aluminum cylinder was accerately turned down to a diameter of 1.738 inches, and then indented in stages. After each incremental load, the diameters of the specimen were measured in the directions of the longitudinal and transverse axes of the Knoop indentation. After an indentation 1.3523 inches long, (nearly the largest size possible with this indenter) the measured diameters had not shown any increase.

4.4 INDENTATION PROCEDURE

The test specimen was initially prepared for repositioning as outlined in 4.2. The smooth test surface was then lubricated and the initial load was applied to the indentation sub-press.

The load was applied at an approximately uniform rate, and when the desired load was reached the unload valve was immediately released. The rate of loading was fast enough to prevent significant creep and slow enough so that the strain rate effects were not considered. All loads were applied with a 20,000 pound Baldwin Testing Machine. The indentation was

then carefully cleaned with a soft cloth and acetone. Extreme care was necessary with the softer metals because any slight abrasion made it very difficult to accurately focus the measuring microscope on the extremities of the indentation.

Using a Leitz measuring microscope, the length of the long diagonal was determined. Before proceeding with the second increment of loading, the indentation was filled with lubricant. Vaseline was used on the tellurium lead and the aluminum, while graphite grease was used on the steel indentations.

Incremental loading, cleaning, and measuring of the diagonal continued until diagonals of the maximum possible size were obtained.

Plan photographs of the indentations formed in four materials, together with a sectional photograph of the same materials are given in Figures 23, 24, 25, and 26. The surfaces formed by sectioning the specimens were etched in an attempt to observe the plastically deformed areas but success was limited.

4.5 EXPERIMENTAL KNOOP NUMBERS

The initial load which is considered to give a reliable Knoop number for a specimen is greater than 100 pounds, and is one which gives an indentation that is at least 0.20 inches long. This was not necessarily the first load on a specimen.

To make possible a direct comparison of the load predicted by theory with the actual load for a given indentation, the data is compiled in the form of graphs in Chapter 5.

(a)

(b)

FIGURE 23 Indentation of annealed mild steel specimen: (a) the indentation, and (b) the cross-section of the indentation. (about 2 1/2 times the actual size)

(a)

(b)

FIGURE 24 Indentation of annealed 0.06% tellurium lead (a) the indentation, and (b) the cross section of the indentation. (about 2 1/2 times actual size)

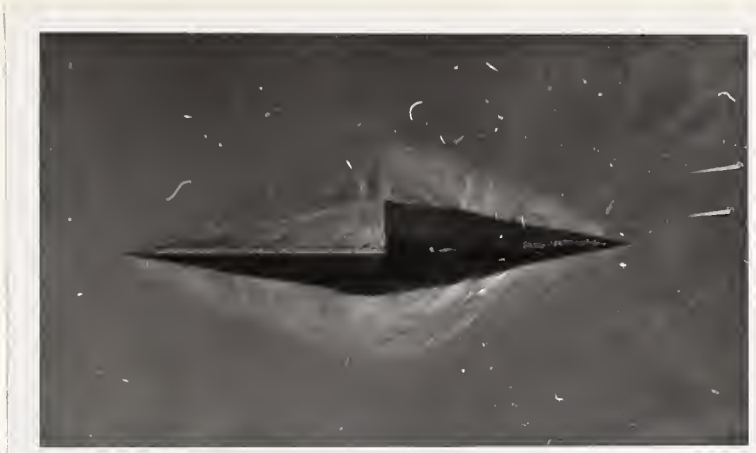

(a)

(b)

FIGURE 25 Indentation of aluminum (conditioned at 570 °F). (a) the indentation, and (b) the cross-section of the indentation. (about 2 1/2 times actual size).

(a)

(b)

FIGURE 26 Indentation of work hardened 0.06% tellurium lead specimen: (a) the indentation, and (b) the cross section of the indentation. (about 2 1/2 times actual size).

CHAPTER 5

A COMPARISON OF THEORY WITH EXPERIMENT

5.1 THE THEORETICAL KNOOP NUMBERS

The theoretical Knoop hardness numbers are the ratio of the theoretical load, F, (equation (31)) to the projected area of the impression. The projected area of the indentation is taken as the area of the original undisturbed surface that has been penetrated by the indenter

The theoretical Knoop number may be shown to be

$$H_k = \frac{k \cot \theta}{2\left[\frac{ck}{F'}\right]} \qquad \text{.....(33)}$$

and it may be seen that it is dependent on θ, and on the coefficient of friction, μ.

The coefficient of friction for vaseline on lead is 0.04 and the quantity ck/F' computed from Grunzweig et al theory on this basis is 0.0368. For the hardened Keewatin steel indenter, $\theta = 64^\circ 54'$, therefore, if k is in kg/mm^2,

$$H_k = 6.3645\ k \qquad \text{.....(34)}$$

"k" is dependent on the value of natural strain that is descriptive of the indentation. Hill[23] suggests that an equivalent plastic strain can be found for the problem of frictionless plane strain wedge indentation by solving the equation

$$e_T = \sqrt{\frac{2}{3}} \sin \theta \sec \left(\frac{\pi}{4} - \theta \right) \quad \ldots\ldots\ldots\ldots\ldots\ldots (35)$$

but at the same time recognizes that this is not too accurate for large wedge angles. For the Knoop geometry, this equation predicts an equivalent strain of 0.79. Tabor[24] obtained a reasonable correllation of Vickers hardness measurements by assuming an equivalent strain of 0.086. Considering such diversity of recommendations, the Knoop hardness numbers were calculated for each of the materials over a possible range of equivalent strains.

5.2 THE RELATIONSHIP BETWEEN THEORY AND EXPERIMENT

Figures 27 through 31 show the relationship between the Knoop numbers (theoretical and experimental) and the load necessary to obtain these numbers.

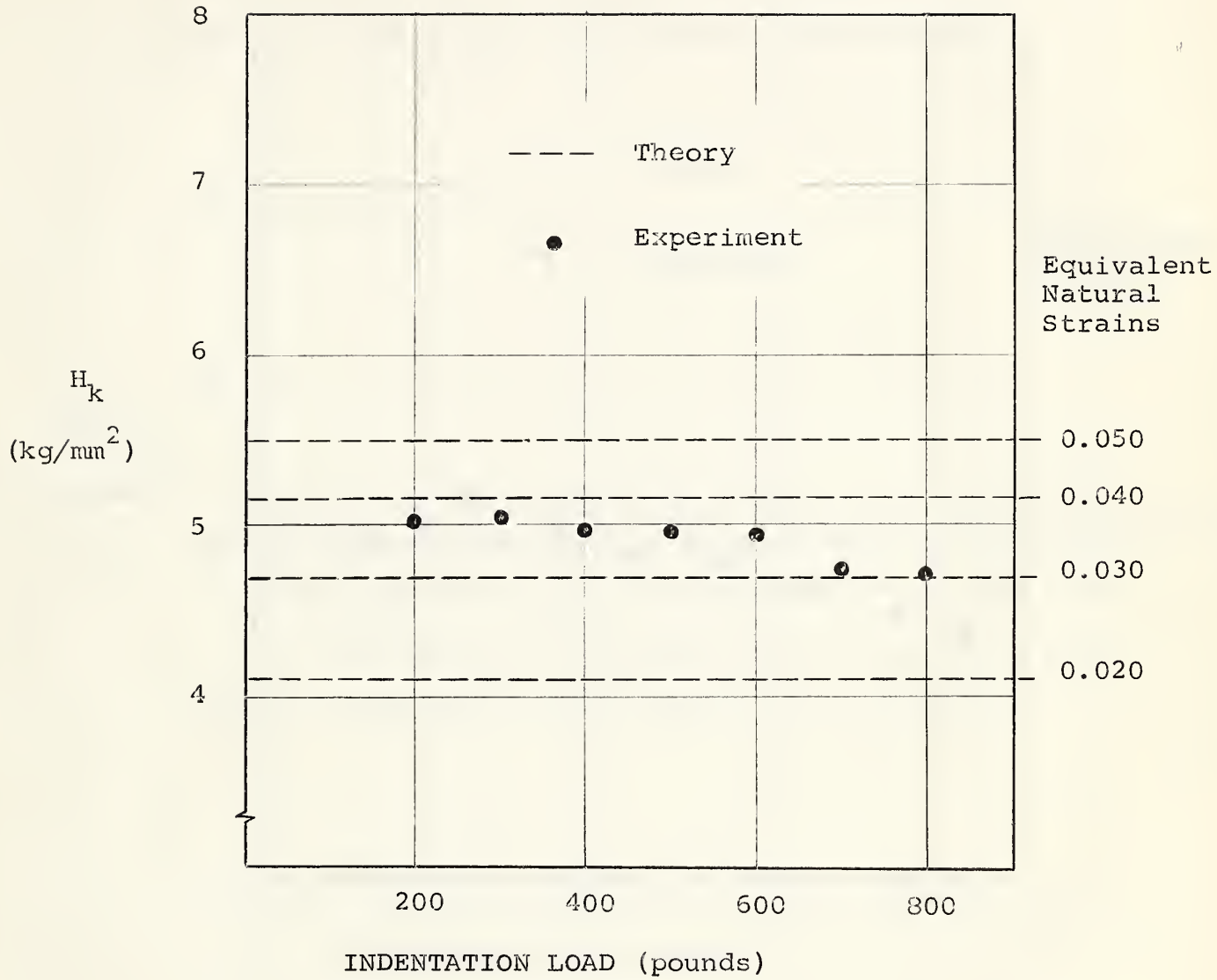

FIGURE 27 Knoop Hardness vs. Indentation Load for 0.06% Tellurium Lead (annealed)

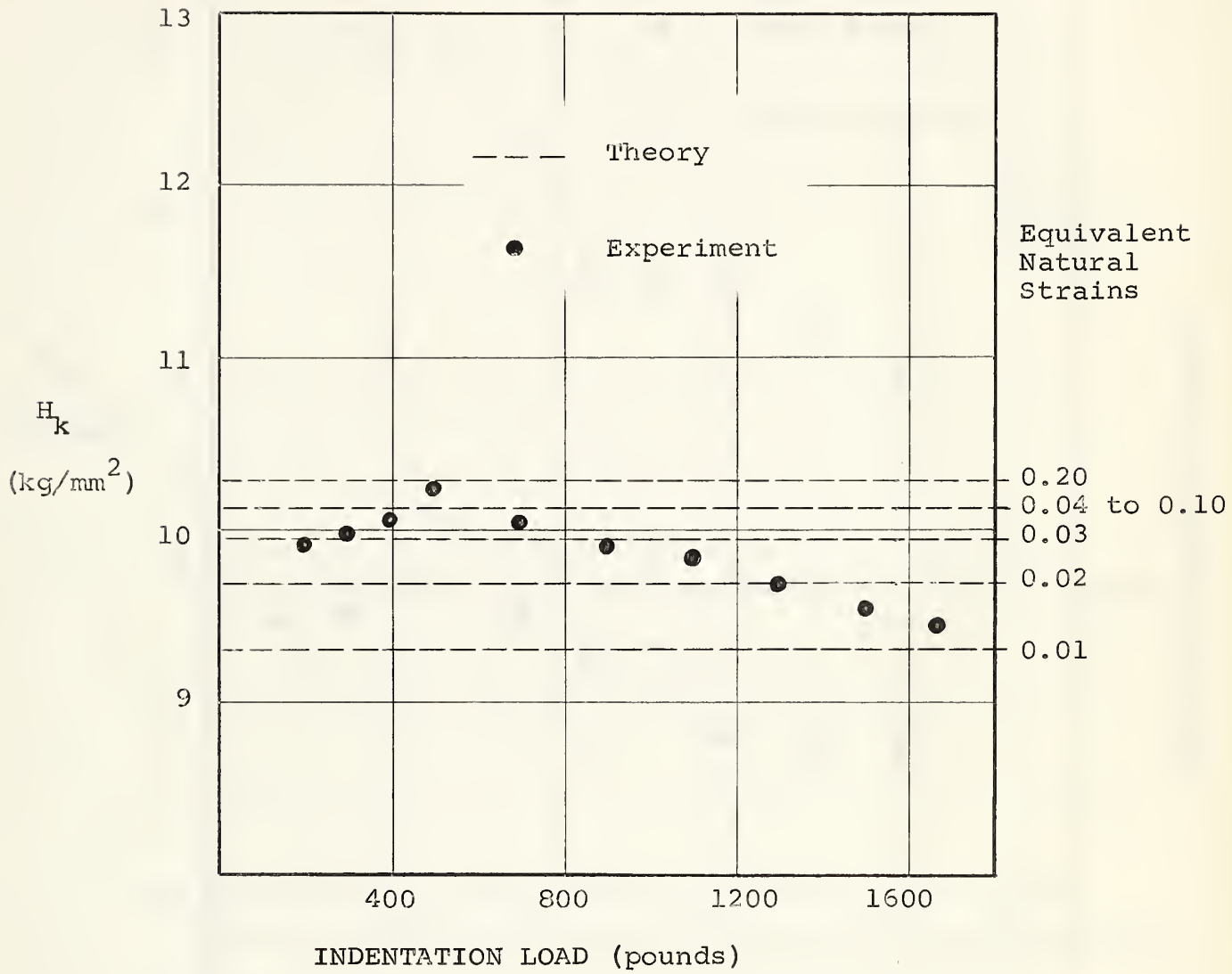

FIGURE 28 Knoop Hardness vs. Indentation Load for 0.06% Tellurium Lead (work hardened)

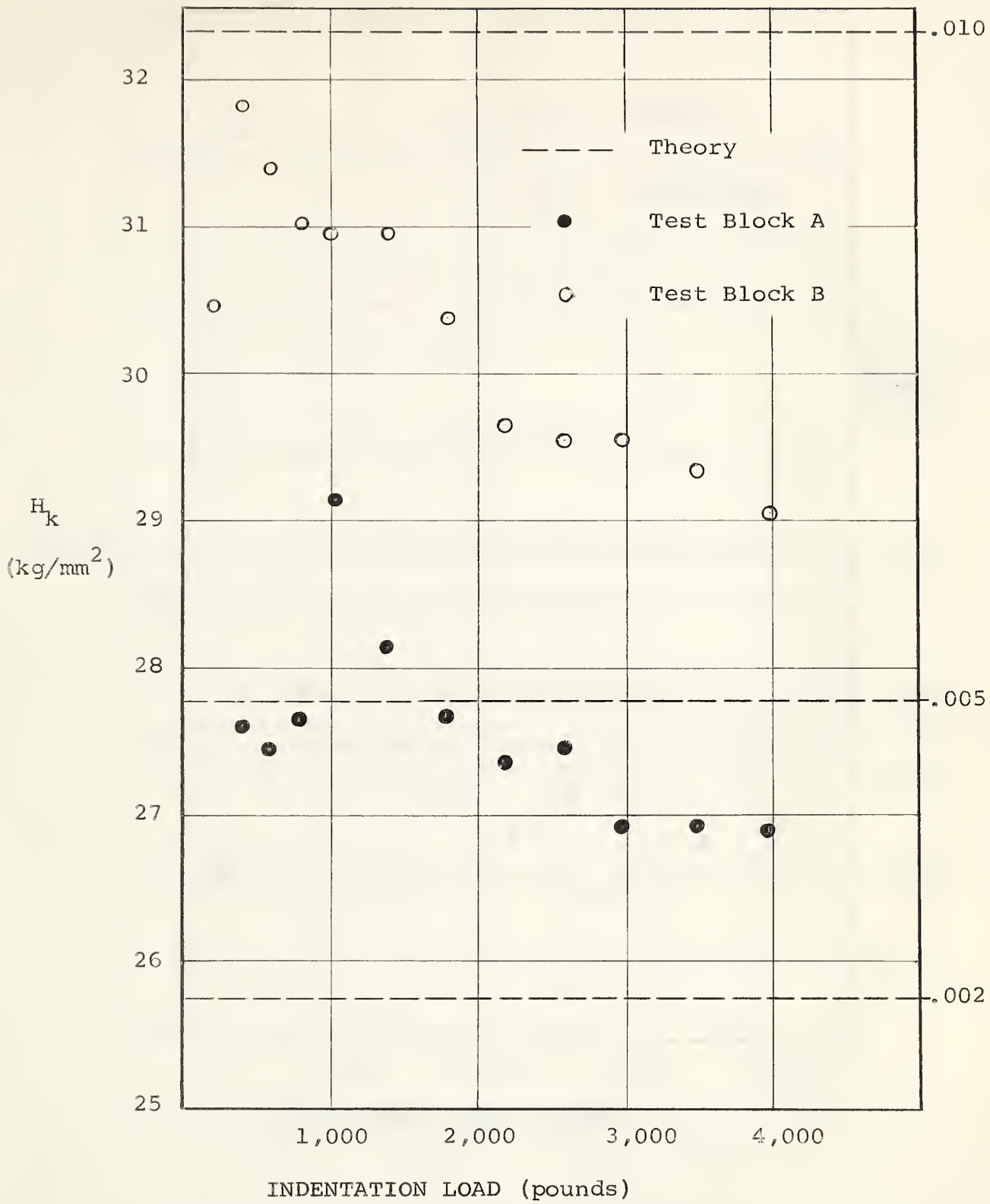

FIGURE 29 Knoop Hardness vs. Indentation Load for Aluminum Test Blocks A and B conditioned at 570°F

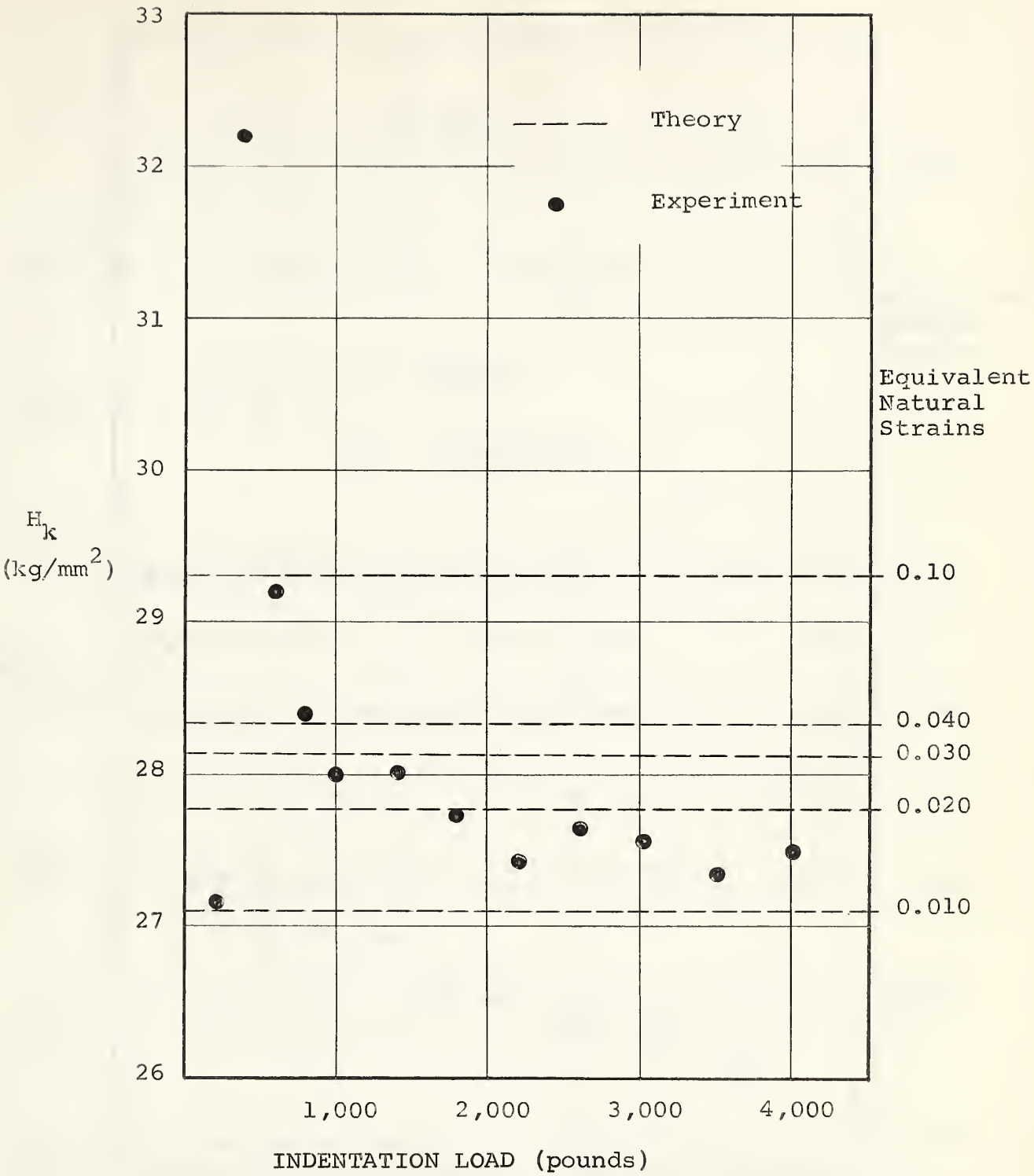

FIGURE 30 Knoop Hardness vs. Indentation Load for Aluminum Test Block C conditioned at 550°F

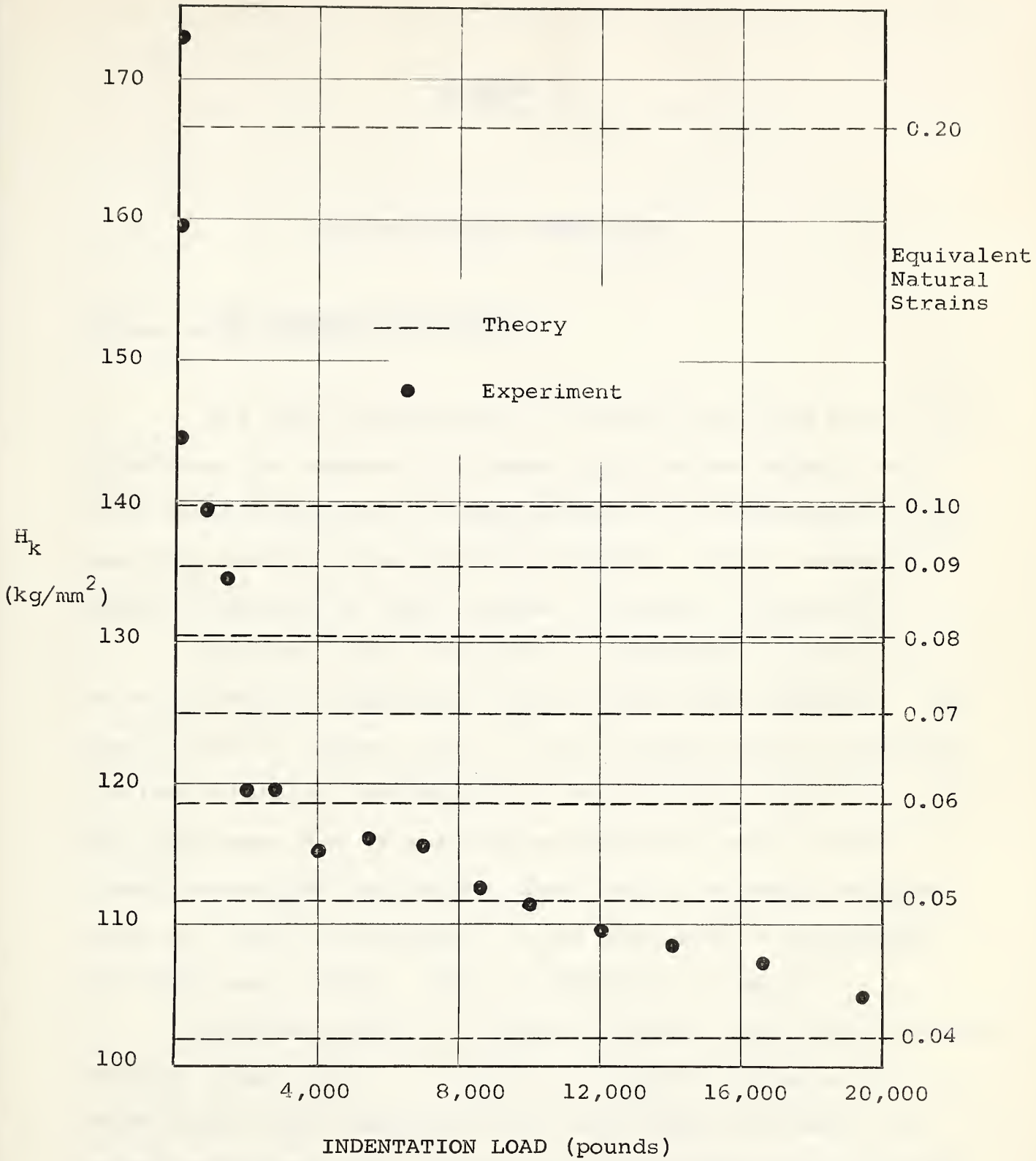

FIGURE 31 Knoop Hardness vs. Indentation Load for 0.20% C annealed mild steel

CHAPTER 6

DISCUSSION AND CONCLUSIONS

6.1 THE COMPRESSION CURVES

The Ford modification of the Cook and Larke method for obtaining the compression stress-strain curves appears excellent in principle, and for hard metals it is undoubtedly faster and more accurate than the Taylor method. Ford's suggestion that lubrication be used, however, is open to objection.

Calcium oleate was used as a lubricant for both the Ford and Taylor compression tests on the steel specimens. For small natural strains (up to 0.14), the Ford curve, supposedly arrived at by the compression of an infinitely long test cylinder and hence free from frictional effects, gave a higher yield stress than the Taylor curve, which, although obtained with the use of lubrication, is not completely uninfluenced by frictional effects. This is difficult to explain.

Calcium oleate is a powder normally, and when compressed becomes greasy and its viscosity may depend on pressure. If each of the four compression cylinders does not undergo the same percentage height reduction for the same load, the areas in contact with the platens will not be identical. It follows

that the pressure would vary from one test cylinder to the other. If the lubrication's viscosity were not pressure dependent, the only effect that it should have on the Ford method is to increase the slope of the constant load lines in Figure 13.

Specimen inhomogeneity may be suggested as a reason for the discrepancy, but all steel compression test cylinders were machined from the same bar stock and were compressed in the same direction so this is unlikely.

The compression curves for annealed 0.06% tellurium lead (Figure 16), obtained without the use of a lubricant, show what theory would predict. The agreement between the two is good.

For metals that are difficult to obtain in an homogeneous state, the Ford method fails to provide even an estimate of the stress-strain relationship. The Taylor method is likewise limited in this case, but it is easier to obtain one homogeneous specimen than four. This was the difficulty that was encountered with the work hardened lead and the aluminum. This is not an insurmountable problem, but it offsets any time advantage that the Ford method may have.

For small strains, say up to 0.05, the Taylor method is probably the least time consuming and almost as accurate as the Ford method. For natural strains from 0.05 to 1.0, the Ford method is more accurate and less time consuming. For strains greater than 1.0, the Taylor method is again the most practical. This is because at or before a natural strain of 1.0, one or two things could have happened. The cylinder with d_o/h_o ratio of 1/2 may have plastically buckled thus rendering

its reduction values meaningless, or, barelling may have become excessive.

The success of the Taylor method is dependent upon arriving at a balance between the desired load increments from a lubricational (ie frictional) point of view, and the desired load increments from an elasticity-plasticity point of view. Increments must be large enough so that the yield strength is identical to that which it would have been if it had been loaded in one operation without the intermediate unloading. For most metals, this should involve an increment of load such that the height is reduced from two to three percent.

6.2 THE KNOOP NUMBERS

The theoretical Knoop numbers are based on the supposition that the material indented is rigid-plastic. The best correlation between theory and experiment should therefore be observed with the metal that has a stress-strain curve that most closely approximates that of a rigid-plastic solid. The work-hardened 0.06% tellurium lead gives the closest approximation.

In Figure 28, with the exception of those for the two highest loads, all the experimental Knoop numbers for this material fall between 9.7 and 10.3. For the work-hardened 0.06% tellurium lead, Y, and hence k, has a constant value over the range of natural strains from 0.04 to 0.10. The theoretical Knoop hardness over this range is calculated to be 10.1.

Theoretical loads for the observed indentations were calculated and they, together with experimental loadings are given in Table II.

Excellent correlation of the two loadings, extending into the micro-indentation hardness range, is observed. The greatest difference between the theoretical and experimental loads is observed at the largest loading and is only 7.2%.

Some generalizations can be made about the Knoop numbers of materials less closely approximated by a rigid-plastic non-hardening solid:

(1) The Knoop number decreases with increasing load. The experimental points are inconclusive as to whether or not an asymptotic value is approached.

(2) There appears to be no equivalent natural strain, common to all specimens, which is descriptive of the Knoop indentation. Both Tate's and Hill's suggested values appear in error.

(3) From micro-indentation data obtained on the same specimens, (not shown in the Figures) it appears that the macro Knoop numbers continue the relationships begun at low loads.

(4) The Knoop numbers for the highest one or two loadings on most specimens appear to drop off abnormally.

If a material does exhibit marked work hardening properties and hence cannot be approximated by the rigid-plastic non-hardening model,the basic difference in the indentation is observed in the form of the pile up. The theoretical load necessary to

A COMPARISON OF THEORETICAL AND EXPERIMENTAL INDENTATION LOADS FOR A MATERIAL APPROXIMATING A RIGID-PLASTIC NON-HARDENING SOLID

TABLE II

KNOOP DIAGONAL	LOADS		
inches	ACTUAL lbs.	THEORETICAL lbs.	H_K (actual)
*.010307	.1102	.1127	10.4
*.01487	.2204	.2346	10.0
*.02099	.4408	.4675	10.0
.4388	200	204	9.9
.5355	300	304	10.0
.6153	400	402	10.1
.6821	500	494	10.3
.8179	700	710	10.0
.9333	900	924	9.9
1.0333	1100	1132	9.9
1.1321	1300	1360	9.7
1.2263	1500	1596	9.5
1.3107	1700	1823	9.5

* Micro Readings

make an indentation of a specified size is of necessity computed on the basis of the rigid-plastic pile up shown in Figure 6. Any slight "sinking in" of the indentation because of a metals capacity for work hardening, will rob the indenter of a portion of the bearing surface which the theoretical load depends upon. It logically follows that the predicted load is much too high in comparison with the observed load unless an unrealistically low equivalent strain is assumed.

The experimental points for the work hardened and annealed 0.06% tellurium lead are averages from two indentation specimens each and the data for the steel are averages from four specimens, one of which was indented without lubrication. This one was used in the average because the Knoop diagonal readings from it were equivalent to those obtained with an equivalent load, from the other three specimens. The effect that an increase in the frictional co-efficient from 0.04 would have is to decrease the value of the parameter ck/F' and hence increase the theoretical load and Knoop number for a given strain. The parameter ck/F' varies from 0.0397 at $\mu = 0$ to 0.0348 at $\mu = 0.164$ (the critical value for the dead metal cap solution).

An interesting possibility is shown by considering Table III which gives detailed parameters calculated by Grunzweig et al for $\theta = 70^{\circ}$ together with data computed on the basis of the dead metal cap solution.

If, during the process of indenting, the coefficient of friction were to increase, as indeed it must because of the

TABLE III

WEDGE INDENTATION PARAMETERS FOR $\theta = 70^\circ$

θ	μ	h/c	P/k	λ	ψ	ck/F'
70°	0	4.34	4.22	45° 0'	63°34'	0.0290
	0.05	4.27	4.45	38°35'	70°50'	0.0275
	0.10	4.21	4.64	31°11'	78°50'	0.0263
	*0.135	4.16	4.75	25° 0'	85°27'	0.0256
	**0.133	3.90	4.82	------	87°23.5'	0.0270

* Solution which Grunzweig called "dead metal cap solution".

** True dead metal cap solution.

virgin metal being exposed at the wedge tip, it is conceivable that ck/F' could "instantaneously" jump from something less than 0.0263 to the critical value of 0.0270. For a fixed load F and shear stress k, this means physically, that the depth of indentation and hence the length of the Knoop diagonal, would increase. This could cause lowering of the Knoop numbers, and give a wide scatter of experimental points. The scatter would depend on whether or not this "snap through" problem occured for each incremental load. The size of the load increment may influence the Knoop numbers. The load increments were generally such that the Knoop diagonal increased approximately 0.05 to 0.10 inches per increment. Since the load varied as the square of the diagonal, increments for larger indentations were two to five times those for smaller indentations. "Snap through" to the dead metal cap solution would occur more readily with larger load increments than with smaller. The generalization that the Knoop numbers for the highest loads generally dropped off could be explained in this manner.

Another possible explanation for the above generalization would be that the specimens were too small, ie the plastic region advanced to the sides. A rough check with a straight edge on the specimen sides indicated that such was not the case.

The data for each aluminum test specimen are given separately (Figures 29 and 30). This was done because correlation between results obtained with specimens prepared in exactly the same manner was impossible. For blocks A and B, conditioned at 570 $^{\circ}$F, the same general trend is exhibited but the Knoop numbers

for a given load differ by approximately two units. This indicates possible anisotropy in the metal. To check for the presence of anisotropy, a new specimen was prepared and indented in stages. The specimen surface was then prepared again by machining off a thickness approximately three times the depth of the last indentation. Indentation about an axis at right angles to the first indentation then proceeded. Results gave a variance in Knoop numbers of similar magnitude to that observable between test specimens A and B.

Much has been said about an elastic recovery factor to account for the decreasing Knoop hardness value with increasing load in micro-indentation hardness testing. Since an elastic recovery factor could only have a magnitude several times smaller than the lengths of indentations produced in this work, it is ruled out as contributing significantly to the lowering observed.

The rate of loading of the test specimens may have affected the Knoop numbers in the cases where a time dependent model is necessary to describe completely the material being used. Further investigations with a programmed loading sequence would be desirable.

In conclusion, direct correlation of theory with experiment is possible only with a material approximating a rigid-plastic non-hardening solid. The work hardening capacity of a metal is considered to be the most serious factor affecting this correlation.

BIBLIOGRAPHY

1. D. Tabor, "The Hardness of Metals", Oxford, Clarendon Press, 1951.

2. B. W. Mott, "Micro-Indentation Hardness Testing", Butterworths Scientific Publications, 1956.

3. F. Knoop, C. G. Peters, and W. B. Emerson, "A sensitive Pyramidal Diamond Tool for Indentation Measurements", Journal of Research, National Bureau of Standards, Vol. 23, July 1939, p. 39

4. Reports of experiments on metals for cannon by officers of the U. S. Ordnance Dept., 1856. (Henry Carey Baird, Philadelphia, Pa.).

5. Reports of experiments on metal for cannon and cannon powder. U. S. Ordnance Dept., 1861. (Chas. H. Crosby, Boston, Mass.).

6. Smith and Sandland, Proc. Inst. Mech. Eng. 1, 623, 1922. Smith and Sandland, J. Iron and Steel Inst. 61, 285, 1925.

7. Knoop et al, op. cit.

8. Knoop, et al, op. cit.

9. D. R. Tate, "A Comparison of Micro-Hardness Indentation Tests", The American Society for Metals, Transactions, Vol. 35, 1945, p. 374.

10. L. P. Tarasov, N. W. Thibault, "Determination of Knoop Hardness Numbers Independent of Load", The American Society for Metals, Transactions, Vol. 38, 1947, p. 331.

11. Mott, op. cit., p. 123.

12. J. Woodrow, A.E.R.E., Harwell, Report ED/R-1, 467, 1954.

13. Notes on Applied Science No. 16, "Modern Computing Methods", H.M.S.O., London, 1961.

14. R. Hill, E. H. Lee, and S. J. Tupper, "The Theory of Wedge Indentation of Ductile Materials", Proc. Roy. Soc. A, 188, p. 273.
R. Hill, "The Mathematical Theory of Plasticity", Oxford U. P., 1950, p. 213.

15. J. Grunzweig, I. M. Longman, and N. J. Petch, "Calculations and Measurements on Wedge Indentations", J. Mech. Phys. of Solids, Vol. 2, 1954, p. 81.

16. Sir G. I. Taylor, Proc. Roy. Soc. A, CXI (1926), p. 531.

17. M. Cook, E. C. Larke, "Resistance of Copper and Copper Alloys to Homogeneous Deformation in Compression", Institute for Metals Journal, Vol. 71, 1945, p. 371.

18. H. Ford, "Advanced Mechanics of Materials", Longmans, London, 1963, p. 651.

19. Tabor, op. cit., p. 55.

20. Knoop, et al, op. cit.

21. N. W. Thibault, H. L. Nyquist, "The Measured Knoop Hardness of Hard Substances and Factors Affecting Its Determination", The American Society for Metals, Transactions, Vol. 38, 1947, p. 313.

22. R. Hill, "A Theoretical Investigation of the Effect of Specimen Size in the Measurement of Hardness", Phil. Mag., Vol. 41, 1950, p. 745.

23. R. Hill, E. H. Lee, and S. J. Tupper, op. cit.

24. Tabor, op. cit. p. 105.